then divided by the mass (mg) of GRK used in each reaction to give the specific activity. For determining ATP K_m values, the data was fit to the Michaelis-Menten equation using Prism v5.0c. For calculating IC_{50} values, the data was fit to log (inhibitor) vs. response with either a fixed or variable slope (Prism v5.0).

Thermofluor Assays

Measurement of protein stability was determined by calculating melting temperatures (T_m) of GRK2 (and other variants) in the presence and absence of ligands. Melting temperatures were determined by monitoring the fluorescence change of 1-anilinonaphthalene-8-sulfonic acid (ANS, Sigma) binding to the hydrophobic interior of the proteins as they denature (*188*). GRK2 or GRK-variants (0.5 mg/mL - 0.2 mg/mL) were incubated at saturating ligand concentrations and 100 μM ANS in a total volume of 10 μL in triplicate, using ABgene 384-well PCR microtiter plates (Thermo-Fisher). Fluorescence was measured at increasing temperatures (4-85°C) in 1 °C intervals using a ThermoFluor 384-well plate reader (Johnson and Johnson). The fluorescence data was analyzed using ThermoFluor Acquire 3.0 software (default settings) and replotted in Prism.

RESULTS

Structures of Native and CMPD1/2-Bound Bovine GRK2-Gβγ

CMPD1 and CMPD2 were co-crystallized with the GRK2-Gβγ complex under similar crystallization and harvesting conditions. The native GRK2-Gβγ complex was co-crystallized with ATP under similar conditions as the inhibitor bound complexes. However, the omit map density for ATP revealed only weak density in the active site, as it was in the original GRK2-Gβγ structure (*174*), and hence it is referred to as the "ligand free" structure, or apoGRK2. The apoGRK2 structure was solved with diffraction data out to 2.67 Å, and the inhibitor bound structures were solved with diffraction data out to 2.50 Å. The diffraction data for all three structures is anisotropic along the *c* axis of the crystals contributing to the poor crystallographic data and refinement statistics for the highest resolution data shells (Table 1).

The apoGRK2 structure superimposes well onto the 1OMW structure with a root mead square deviation (rmsd) of 0.35 Å for 614 Cα positions. The binding of both CMPD1 and CMD2 induce conformation changes in the active site of GRK2 with an rmsd of 0.6 Å and 0.5 Å (for 290 Cα positions in the kinase domain) for CMPD1 and CMPD2, respectively (Table 3). Qualitatively, CMPD's 1 and 2 induce conformational changes that are nearly identical to that of balanol (Table 3). For CMPD's 1 and 2, subtle conformational changes are observed in the P-loop and αB-αC helices, in which individual atoms move up to 0.8 Å and 0.9 Å, respectively (Figure 33A-D). The binding of CMPD1 and CMPD2 also cause a

slight closure of the large lobe relative to the small lobe of 3.6° and 2.4°, respectively.

Table 2: Crystallographic data and refinement statistics

Ligand: X-ray Source:	apoGRK2 APS 21-ID-G	CMPD1 APS 21-ID-G	CMPD2 APS 21-ID-G
Wavelength (Å)	0.9786	0.97856	0.97856
D_{min} (Å)	2.67 (2.76-2.67)	2.5 (2.59-2.5)	2.5 (2.59-2.5)
Space Group	C2	C2	C2
	b = 73.2	*b* = 74.3	*b* = 73.5
	c = 122.8	*c* = 123.3	*c* = 122.0
	β = 115.4°	β = 115.7°	β = 115.1°
Unique reflections	43,102 (4,259)	50,352 (5,303)	51,786 (5,149)
Average redundancy	4.0 (4.0)	3.8 (3.8)	6.4 (6.5)
R_{sym} (%)[a]	7.3 (58.8)	7.2 (>100)	8.5 (>100)
Completeness (%)	99.6 (99.8)	94.2 (100)	99.1 (98.6)
$\langle I \rangle / \langle \sigma_I \rangle$	15.7 (2.6)	20.45 (1.16)	16.4 (0.9)
Refinement resolution	30-2.67 (2.74-2.67)	30-2.49 (2.56-2.49)	30.0-2.48 (2.54-2.48)
Total refelctions used	40,908 (2,955)	47,727 (3,539)	49,091 (2,573)
Protein atoms	8,117	8,085	8,072
Non-protein atoms	16	80	62
RMSD bond lengths	0.001	0.009	0.014
RMSD bond angles	1.2	1.1	1.1
Est. coordinate error	0.6	0.3	0.4
Ramachandran most favored, disallowed (%)	89.8, 0.0	89.4, 0.0	90.0, 0.0
R_{work}[b]	22.2 (32.0)	23.7 (36.7)	22.6 (37.2)
R_{free}[c]	25.7 (42.2)	28.5 (41.7)	27.4 (33.8)
PDB Entry	TBD	TBD	TBD

[a] $R_{sym} = \Sigma_{hkl}\Sigma_i |I(hkl)_i - I(hkl)| / \Sigma_{hkl}\Sigma_i I(hkl)_i$, where I(hkl) is the mean intensity of *i* reflections after rejections. R_{sym} values for CMPD1 and CMPD2 in the highest resolution shell are greater than 100% due to anisotropic diffraction.

[b] $R_{work} = \Sigma_{hkl}||F_{obs}(hkl)| - |F_{calc}(hkl)||/ \Sigma_{hkl}|F_{obs}(hkl)|$; For CMPD2 the high resolution shell $R_{work} > R_{free}$ suggesting the data in the shell is under refined, again due to anisotropic data.

[c] 5% of the truncated data set was excluded from refinement to calculate R_{free}.

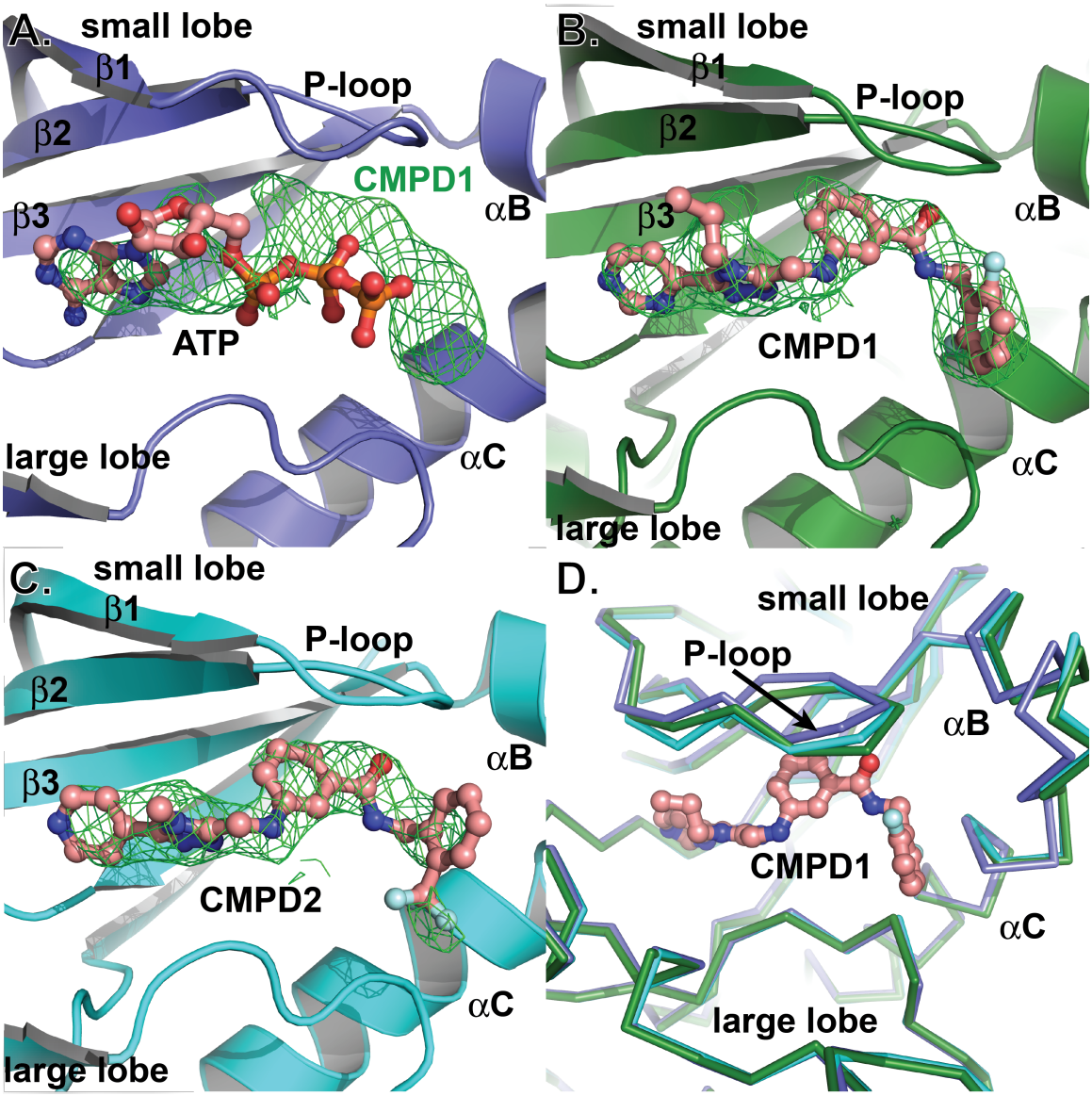

Figure 33: Crystal structures of inhibitor bound GRK2. All ligands are shown as a ball and stick model with carbons colored pink, nitrogens blue, oxygens red, phosphates orange, and fluorines white. Electron density (green) is shown for the $|F_o|$ - $|F_c|$ omit map contoured at the 3σ level. **A)** An active site view of the apoGRK2-Gβγ. ApoGRK2 is shown in slate blue with ATP modeled from the GRK1 structure (PDB: 3C4W), electron density is that of CMPD1 and shows significant overlap for the binding sites of the two compounds. **B)** CMPD1

and **C)** CMPD2 bound in the active site of GRK2. Like Balanol, CMPD1 and 2 are active site, competitive inhibitors. **D)** Comparative Cα trace of the apoGRK2 (blue) structure with the Cα traces of CMPD1 (green) and CMPD2 (cyan). Significant changes are observed in the P-loop and in the αB-αC loop. The entire GRK2 sequence was used for the superpositions in this figure.

Table 3: Conformational changes of ligand bound GRK2. The binding of CMPD1/2 induce similar conformational changes in the kinase domain as seen in the balanol structure.

Ligand:		Balanol [a]	CMPD1[b]	CMPD2[b]
	residues:		rmsd (Å)	
Small lobe	186-272	0.5	0.4	0.5
Large lobe	273-475	0.3	0.4	0.4
Kinase domain	186-475	0.6	0.6	0.5
P-loop	191-211	0.5	0.3	0.4
αB-αC helices	224-246	0.5	0.3	0.4
Large lobe closure [c]		4.0°	3.6°	2.4°

[a]Balanol (PDB: 3KRW) was superimposed against human GRK2-Gβγ (PDB: 3CIK).
[b]CMPD1 and CMPD2 were superimposed against apoGRK2.
[c]Domain closure of the large lobe was calculated relative to the small lobe.

Compound Binding

Like balanol in the hGRK2·balanol-Gβγ structure, CMPD1/2 binds deep in the active site of GRK2, overlapping the binding site for ATP (Figure 33A-C). The ATP binding site is composed of several binding-pockets including the adenine, ribose, triphosphate, and hydrophobic subsites. The adenine subsite is relatively hydrophobic in nature, and the N1 atom of adenine (from ATP) forms a hydrogen bond with the backbone nitrogen and the N6 atom forms a hydrogen bond with the backbone carbonyl oxygen of residues in the hinge (Met274 and Asp272,

respectively, in GRK2). In our structures, the A ring of CMPD's 1 and 2 occupy the adenine subsite with the N4 atom forming a weak hydrogen bond with the backbone amide hydrogen of Met274 at a distance of 3.7 Å apart (Figure 34A).

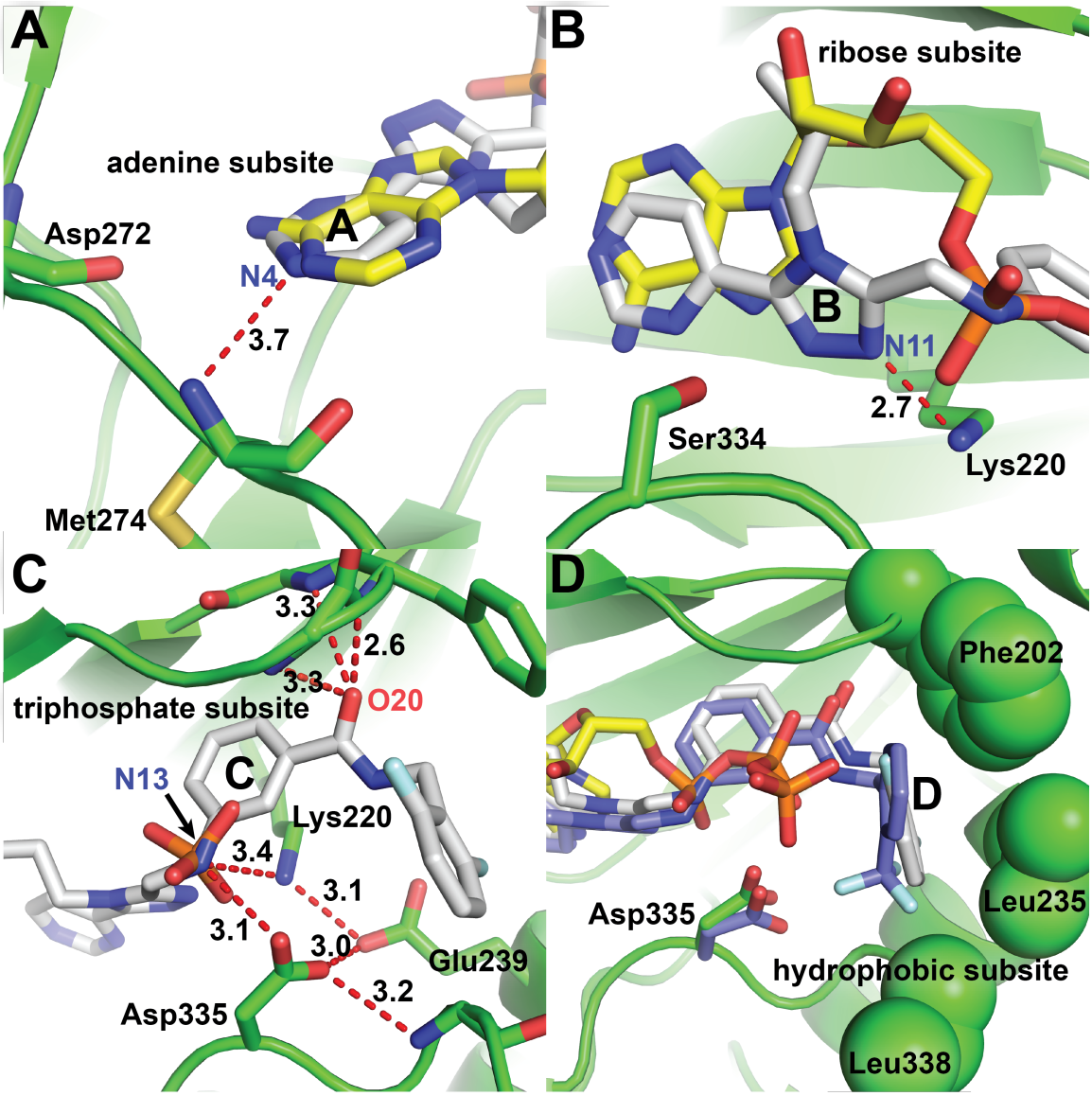

Figure 34: Structural analysis of the ATP subsites. All ligands are shown as sticks with nitrogens colored blue, oxygens red, fluorines white, phosphates orange, sulfur yellow and the carbons from ATP yellow, CMPD1 white, and

CMPD2 slate. ATP is modeled from PDB: 3C4W. Some regions of the structure are not shown for clarity. All distances shown are in units of Ångstroms. **A).** The adenine subsite. The adenine-binding site is generally characterized by two hydrogen bonds to the hinge region. CMPD1/2 are in position to form a hydrogen bond with the backbone nitrogen of Met274. **B)** The ribose subsite. The N11 atom on ring B of CMPD1/2 forms a hydrogen bond with Lys202. There is also a van der Waals contact between Ser334 and the triazole ring of CMPD1/2. **C)** The triphosphate subsite. Numerous interactions are observed in the triphosphate subsite including both the P-loop and the activation loop. **D)** The hydrophobic subsite. Ring D of CMPD1/2 bind in the hydrophobic subsite which is a pocket formed by the αC helix and the activation loop. Type II kinase inhibitors that target inactive kinase conformations utilize this subsite (*189*).

The ribose subsite in our structures is partially occupied by the 1,2,4-triazole moiety (ring B; Figure 34B). The triazole structure sits farther back into the binding site than ribose, and forms a hydrogen bond to Lys220. Nonpolar interactions between the substituted triazole and GRK2 include residues Ile197, Val205, Leu271, and Ser335.

The C ring of CMPDs 1/2 is positioned in the triphosphate subsite with the amino group (N13) occupying the site of the α-phosphate and the benzamide oxygen (O20) positioning itself under the P-loop (Figure 34C). The amino group (N13) forms a hydrogen bond with both Asp335 and Lys220. There is chain of

hydrogen bond interactions between Lys220, Glu239, Asp335, and Gly337. The carbonyl oxygen (O20) is also positioned under the P-loop and is within hydrogen bond distance to three-backbone amide nitrogens from residues Gly201, Phe202, and Gly203 (Figure 34C). This P-loop interaction is very similar to that of the benzophenone ring C of balanol, which forms several hydrogen bonds with backbone atoms of the P-loop (*190*).

The D ring of CMPDs 1/2 binds in the hydrophobic subsite (also referred to as an allosteric site) that is formed by residues in the P-loop, αB-αC helices, and the activation loop. This pocket has become a major target for creating selective kinase inhibitors, as compounds that bind in this site seem to stabilize a unique inactive kinase conformation (examples include: imatinib, BIRB796, and sorafenib (*189*)).

Determination of CMPD1/2 Selectivity Against GRK1, GRK2, and GRK5

The Takeda patent (*176*) reported that CMPDs 1/2 are selective inhibitors for GRK2 versus PKC, PKA, and ROK. However, they lacked data on the selectivity of between members of the GRK family. As a control, we first tested the activity of balanol against GRK1, GRK2, and GRK5. Balanol had an IC_{50} of ~40 nM for GRK2, similar to previously reported values (*175*). Surprisingly, balanol showed moderate selectivity towards GRK5 and GRK1, with IC_{50} values of ~400 nM and ~4 μM, respectively (Figure 35A, Table 4). These IC_{50} values differ from the previously reported values (*175*) of 160 nM (GRK5) and 340 nM (GRK1),

possibly due to different assay conditions (e.g. receptor substrate and/or ATP concentrations). We then tested CMPDs 1/2 against GRK2 yielding IC_{50} values of ~50 nM and ~200 nM, respectively (Figure 35B, Table 4), similar to the values reported in the patent. Next we tested CMPDs 1/2 against GRK1 and GRK5. Both CMPDs show no activity towards inhibiting GRK1 and GRK5 at the concentrations tested (up to 125 μM). Thus, CMPD1 and 2 are specific for GRK2 under these conditions.

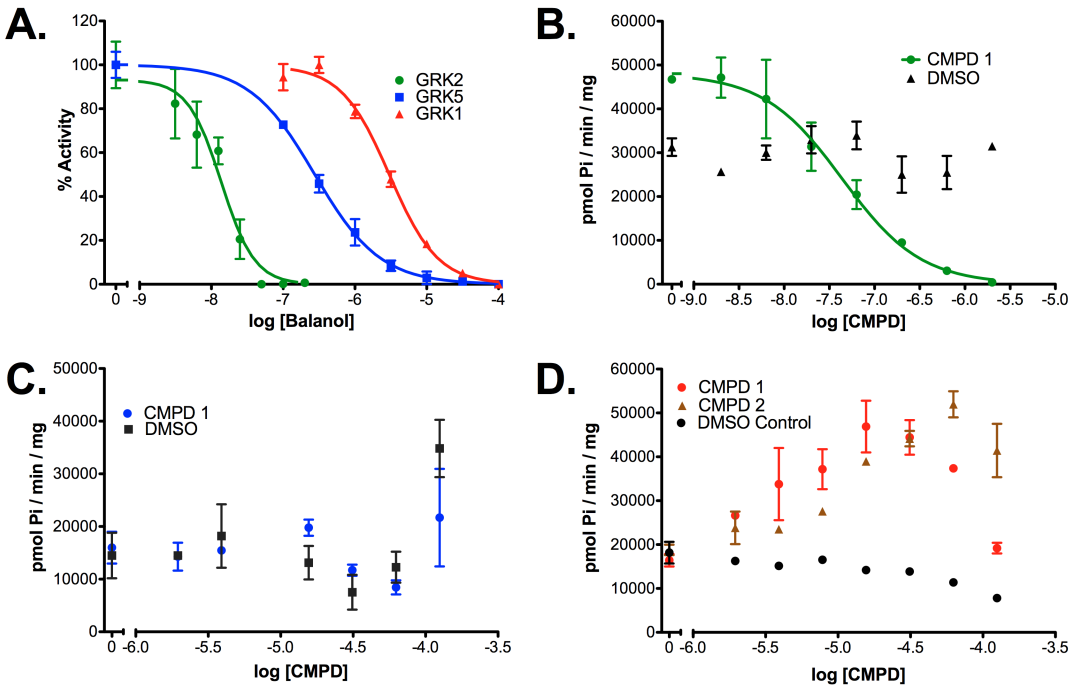

Figure 35: Inhibition of rhodopsin phosphorylation by small molecules. A) Inhibition of GRK1, GRK2, and GRK5 activity by balanol. IC_{50} values of approximately 40 nM, 400 nM, and 4 μM (n≥3, in duplicate) were determined for GRK2, GRK5, and GRK1, respectively. Inhibition of **(B)** GRK2, **(C)** GRK5, and **(D)** GRK1 activity by CMPD1 or, as a control, DMSO. The IC_{50} of CMPD1 against GRK2 is approximately 50 nM. CMPD1 and 2 do not inhibit GRK5 or

GRK1 activity at the tested concentrations (≤125 μM CMPD; 0.5 mM ATP). Additional curves for CMPD1/2 against GRK2 can be found in **Figure 39**C-F. The results show mean ± SEM values, run in duplicate, from a representative experiment.

Analysis of the GRK2 Inhibitor Binding Site

The binding of balanol, CMPD1, and CMPD2 appear to induce very similar conformational changes in the active site of GRK2. However, our previous data strongly indicates that CMPDs 1/2 are significantly more selective towards GRK2 than balanol (Figure 35). In general, residues around the inhibitor/ATP-binding site are very well conserved among AGC kinases. Based on our crystal structures and homology modeling (Figure 36) we identified five amino acids around the inhibitor-binding site that may contribute to the inhibitor selectivity by making unique contacts to the Takeda compounds.

Previous work by Breitenlechner *et al.* showed that PKA to PKB amino acid exchanges in the active site could confer inhibitor selectivity among balanol-like derivatives (*191*). Specifically, the PKA to PKB mutations F187L and Q48E (corresponding to residues Leu338 and Gly232 of GRK2, (Figure 34D) which help form the hydrophobic subsite) enabled them to generate PKB selective inhibitors. In GRKs the analogous two residues Leu338 and Gly232 are invarient (Figure 36). However, the adjacent residue Leu235 is a glycine in GRK1, and a methionine in GRK4, -5, -6, and -7. Furthermore, in our inhibitor-bound

structures (Figure 37B) Leu235 adopts a different rotamer conformation to accommodate the binding of the D ring. Hence, Leu235 was selected for mutagenesis studies on the basis that it could form selective interactions with the D ring of CMPDs 1/2.

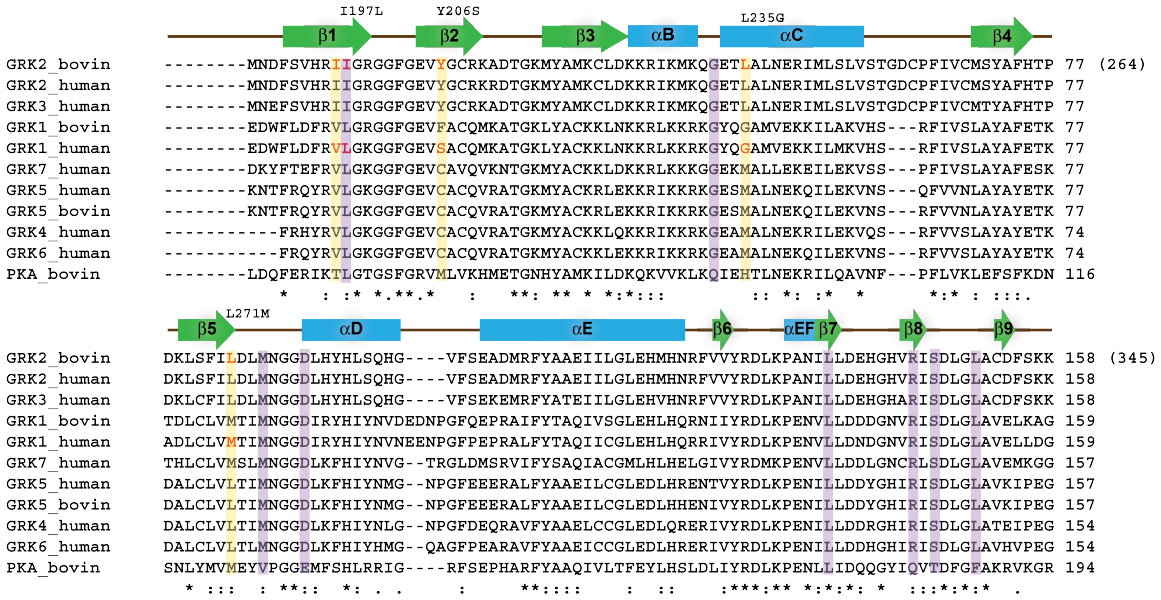

Figure 36: Sequence alignment of the GRK subfamily kinase domain. The kinase domain of human GRK1-7, bovine GRK1-7, and bovine PKA were aligned using the ClustalW server (residues 189-345 shown, GRK2). Residues colored purple correspond to positions in either PKA or PKB that have been previously mutated to assess mechanisms of selectivity. Residues colored yellow and red were selected for our mutagenesis studies of GRK2.

In other work, researchers investigated the molecular basis for selectivity in inhibitors that bind to PKA mutants of Rho-kinase (*192*). Non-conserved residues in the P-loop, hinge region, and activation loop were selected for mutagenesis, and two Rho-kinase residues Ala183 and Ile49 were shown

(corresponding to residues Ser334 and Ile197 in GRK2) to be determinants of Rho-kinase inhibitor binding specificity.

Sequence alignment (Figure 36) between the various GRK isoforms revealed non-conserved residues in close proximity to the inhibitor-binding site. Some of these residues are found in the P-loop, including Ile197, which is at the analogous position to the PKA-L49I mutation. Furthermore, non-conserved positions in the P-loop (I196, I197, and Y206) undergo the most significant conformational changes in our inhibitor bound structures compared to apoGRK2 (Figure 37A). Thus, the following mutations were hypothesized to decrease the affinity of the inhibitors for GRK2 by converting them to their equivalents in GRK1: I196V, I197L, and Y206S. Additionally, the so-called “gatekeeper residue”, which sits at the back of the adenine subsite has been shown to be a major determinant for kinase inhibitor specificity (*172*), and is non-conserved between GRK2 and GRK1/GRK7 (Figure 36). Thus the L271M mutant was additionally selected.

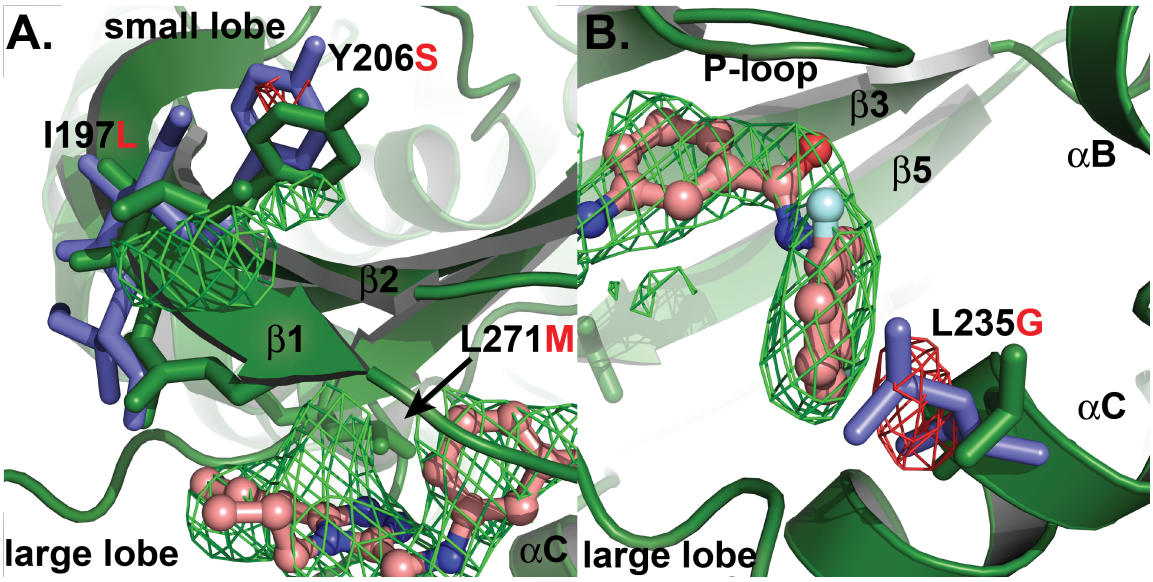

Figure 37: Conformational changes in the P-loop and αB-αC helices. Electron density is shown for a $|F_o|–|F_c|$ omit map of GRK2·CMPD1-Gβγ contoured at the 3σ level with positive density shown in green and negative in red. The labeled residues correspond to bovine GRK2 with the analogous human GRK1 residue indicated in red. **A)** Non-conserved residues in the P-loop and hinge region selected for mutagenesis. **B)** Displacement of residue Leu235 upon compound binding. Residues from the apoGRK2 structure are colored slate, and residues from the GRK2·CMPD1-Gβγ structure are colored green.

Determination of Inhibitor Selectivity via GRK2 Mutations

The GRK2 mutations I197L, Y206S, L235G, and L271M were made in the background of the bovine GRK2-S670A-H_6 construct and protein was purified to homogeneity from baculovirus-infected insect cells. The I196V mutant would not stably express and was not further studied. For comparison of inhibitor

selectivity against the other GRK subfamilies, bovine $GRK1_{535}$-H_6 (GRK1) and bovine $GRK5_{561}$-H_6 (GRK5) were used. To test the ability of our inhibitors to inhibit the kinase activity of our GRK constructs, we performed phosphorylation assays using bovine rod outer segments (bROS) as the receptor substrate and ATP at saturating concentrations (0.5 mM). Assays were performed with a single time point within the linear range of enzymatic activity (Figure 32). Dose-response curves were fit to both a three-parameter (fixed hill slope) or four-parameter (variable hill slope) dose-response curve using Prism 5.0c. In general, the three-parameter model fit the data well, however, some curves required a four-parameter fit.

Prior to testing the activity of our inhibitors against the GRK2 mutants, we determined the ATP K_m values for GRK1, 2, 5, and for each mutant. We did not expect the mutated residues to alter the K_M values as all GRKs are optimized to use ATP, and hence the substitutions are not anticipated to change ATP binding or hydrolysis. Indeed, our K_m values for ATP were similar to previously reported values for GRK1, GRK2, and GRK5 (Figure 38). The GRK2 mutants had similar K_m values to GRK2, allowing us to directly compare IC_{50} values for the various GRK2 mutants. It should be noted that GRK1 and GRK5 have slightly differing K_m values for ATP, resulting in K_i values for balanol of approximately 2 nM, 30 nM, and 100 nM for GRK2, GRK5, and GRK1, respectively. Thus, balanol is indeed selective. However, it is still a relatively potent inhibitor for all three GRK subfamilies.

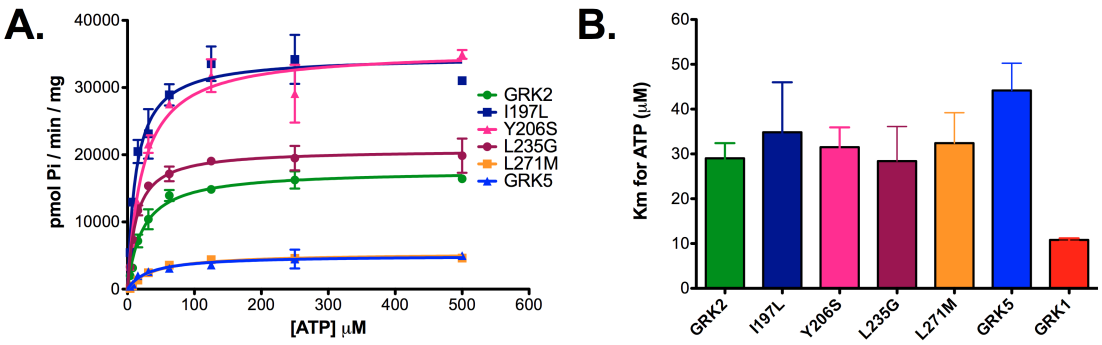

Figure 38: GRK K_m values for ATP. A) K_m values for ATP were determined by measuring phosphorylation of bROS. Data is fit to the Michaelis-Menten equation using Prism 5.0c to determine K_m values. Data for GRK1 is not shown. **B)** Summary of K_m values for each GRK protein. The K_m values among the GRK2 mutants are not significantly different. The results shown are mean ± SEM values, run in duplicate, from a representative experiment (n≥3).

Next, we tested the ability of balanol to inhibit the GRK2 mutants (Figure 39A,B). The IC_{50} values for balanol showed little difference between wild-type GRK2 and the I197L, Y206S, and L235G mutations (Table 4). Surprisingly, the gatekeeper mutation L271M increased the potency of balanol by 10-fold, further supporting the importance of the gatekeeper residue in modulating inhibitor binding. It is structurally unclear as to why this mutation would increase the potency of balanol, but it could be due to reordering of amino acids around the hinge region that create more favorable hydrophobic contacts with the A ring.

As for balanol, the P-loop mutations I197L and Y206S have no net affect on CMPD1 or 2 binding to GRK2 (Figure 39C-F). This is contrast to the previous

PKA-L49I mutation, which substantially (~180 fold) decreased the affinity of the staurosporine like inhibitor KT5720 (*192*). The lack of an affect of the I197L mutant could impart be do to the lack of the neighboring I196V mutation, which together could significantly alter the binding-site.

The L235G mutation in the αB-αC loop caused a 2-3 fold decrease in the potency of CMPDs 1/2, indicating that the hydrophobic subsite in GRKs may play a role in contributing compound selectivity. Indeed, previous studies with PKA and PKB showed that differing residues around the "benzophenone pocket" of balanol could be used to design selective inhibitors (*191*). While a two-to-three fold shift in potency is not enough to fully explain the degree of selectivity achieved by CMPDs 1/2, it does suggest that further investigation of substitutions in the αB-αC helices could be warranted. For example, the L235M mutation would be interesting due to the possibility of a steric collision with the inhibitor due to the slightly longer side chain of methionine.

The L271M mutation appeared to slightly increase the potency of CMPD1 and decrease the potency of CMPD2 (Figure 39D,F). Although neither result is statistically significant, it is interesting that the A ring of CMPD1 is a pyrimidine ring, in which the N2 atom could be involved in a favorable electrostatic interaction with the sulfur atom on the methionine residue. Regardless, the gatekeeper residue appears to have little influence on the affinity of GRK2 for CMPDs 1/2.

Table 4: IC_{50} values of GRK inhibitors against bROS phosphorylation. All experiments were performed with 5-20 μM bROS, 50 nM GRK, and 0.5 mM ATP at a 5-10 minute time point at ~25°C. Values shown represent means ± S.E. from three to five experiments run in duplicate.

GRK	Balanol (nM)	CMPD1 (nM)	CMPD2 (nM)
GRK2	39 ± 9	45 ± 15	200 ± 92
-I197L	31 ± 16	78 ± 17	323 ± 42
-Y206S	22 ± 5	57 ± 13	251 ± 43
-L235G	29 ± 14	129 ± 30	471 ± 49
-L271M	4.3 ± 1	21 ± 3	368 ± 55
GRK5	380 ± 110	ND[a]	ND[a]
GRK1	4.4 ± 0.7 μM	ND[a]	ND[a]

[a]ND, not detectable. No inhibition was observed at the concentrations tested.

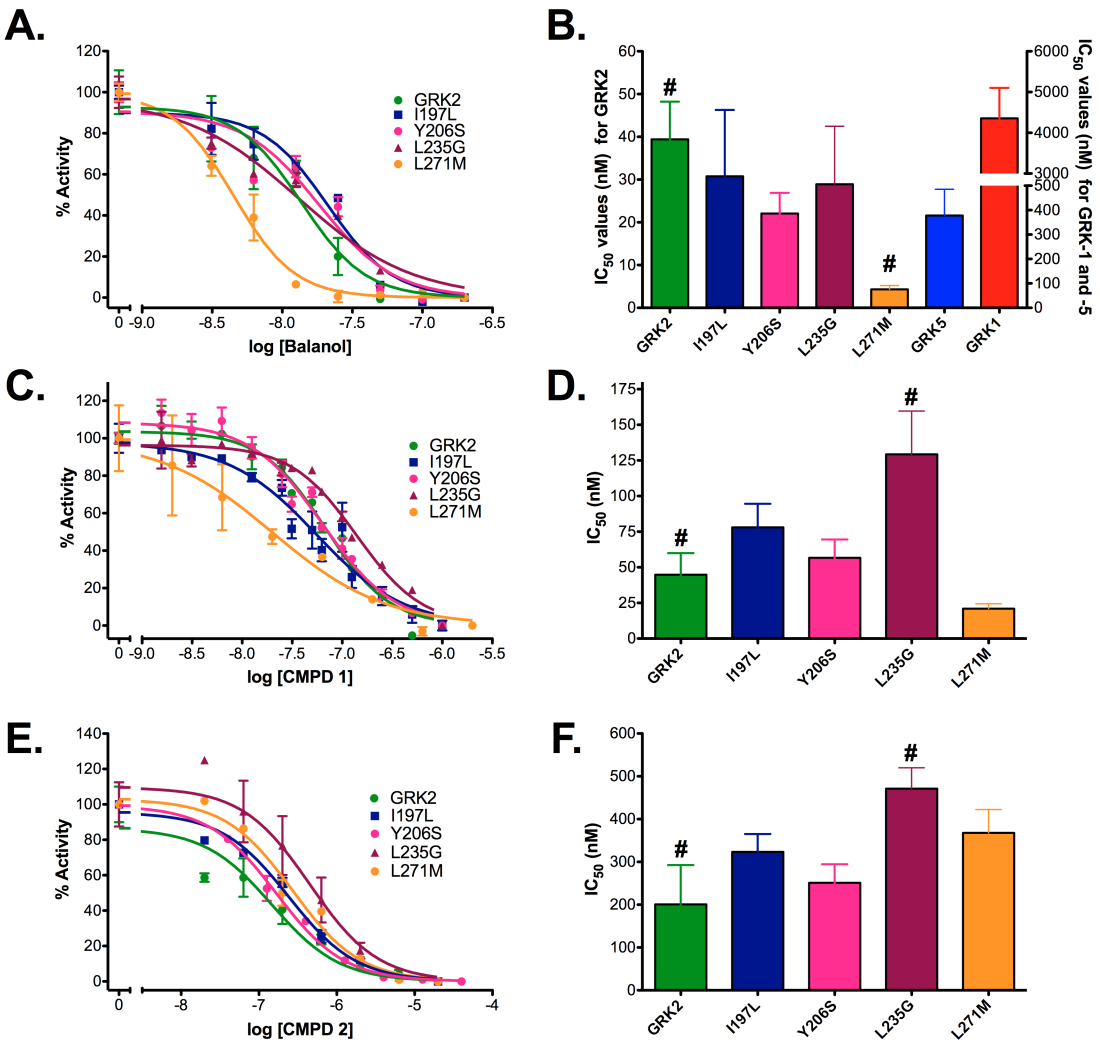

Figure 39: Inhibition of active site mutants of GRK2. Inhibition of GRK2 activity towards rhodopsin for **A-B)** balanol, **C-D)**, CMPD1, and **E-F)** CMPD2. Dose-response curves were fit to either a 3-parameter or 4 four-parameter model to determine IC_{50} values. Experiments were performed in duplicate with n≥3 separate experiments for each mutant and inhibitor. Column's labeled with **#** are statistically significant ($p<0.05$) as determined by one-way ANOVA with a Dunnett post-test compared to GRK2.

Determination of Ligand Induced Protein Stability

We were interested in comparing the results from our inhibition data (Table 4) with the ability of our inhibitors to thermally stabilize GRK2, GRK2-mutants, GRK1, and GRK5 to determine if the increase in GRK1 activity due to CMPDs1/2 (Figure 35) could be due to thermal stabilization. The binding of a ligand to a protein only occurs if there is a release of free energy as described by the Gibbs free energy equation $\Delta G° = RTlnK_d$. Thus, a protein-ligand complex is more stable than free protein. Thermal denaturation of a protein can be determined by measuring the fluorescence change of a fluorophore that preferentially binds to the denatured state of the protein. Ligand binding to the native-protein state will cause a stabilization of the protein that depends on the binding energy of the complex, and can be described as a rightward shift in a thermal denaturation curve (ΔT_m) (*193*).

Native GRK2 has a melting temperature (T_m) of approximately 37°C, and the addition of 500 μM ATP results in a 5 °C increase in its T_m indicating that the binding of ATP stabilizes GRK2, as expected. 20 μM balanol, 100 μM CMPD1, and 100 μM CMPD2 further increase the stability of GRK2 with ΔT_m values of 19°C, 16.0°C, and 12°C, respectively (Figure 40). These ΔT_m values are identical to the rank order of the compounds potency for inhibiting kinase activity, suggesting that the thermal stability assay can give valid comparisons of ligand affinity and, possibly, selectivity.

We next tested the thermal stability of GRK1 and GRK5 (Figure 40). Both GRK1 and GRK5 have significantly lower melting temperatures of 27°C and 29°C, respectively (Figure 41E,F). When bound to ATP, GRK1 is stabilized by an additional 15°C which is significantly more than the ~6°C stabilization for GRK2. The T_m of GRK5 is increased by ~8°C, similar to GRK2. These results correlates well with both the lower ATP K_m values for GRK1 versus GRK2 and the similar ATP K_m values exhibited by GRK5 and GRK2 (Figure 40).

Surprisingly, balanol is less affective than ATP in thermostabilizing GRK1 and GRK5 with T_m shifts of only ~10°C and ~6°C. Furthermore, CMPDs 1/2 are even less affective than balanol with ΔT_m values of approximately 6°C and 3°C for GRK1, and 3°C and 2°C for GRK5, respectively. Thus, CMPDs 1/2 do appear to bind and slightly stabilize both GRK1 and GRK5. In our phosphorylation assays, it was observed that CMPDs 1/2 actually increase the catalytic activity of GRK1, although higher concentrations do negate the effect (Figure 35C,D). This can be explained by the thermal stability of GRK1, which has a T_m close to room temperature. Upon CMPD1 binding, the T_m is shifted to 33°C stabilizing the protein and consequently the kinase activity before the assay is started with the addition of ATP and light. Overall, the thermal stability data indicates that the selectivity achieved by balanol, CMPD1, and CMPD2 is the result of greater thermostabilization of the kinase domain for GRK2 than for GRK1 or GRK5, which reflects less temperature-dependent fluctuations in GRK2 complexes and a better fit to the inhibitor.

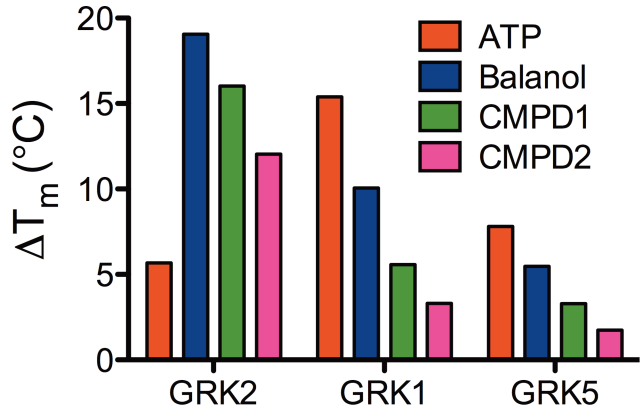

Figure 40: Comparison of thermal stability changes for GRK isoforms. The change in melting temperature (ΔT_m) was calculated by subtracting the unbound T_m from the ligand bound T_m. The concentration of ATP in this assay is 500 μM for all samples. Balanol is at 20 μM for GRK2 and 200 μM for GRK1 and GRK5. CMPD1 and 2 are 100 μM for all GRKs. Data is representative of two to three independent experiments performed in triplicate.

We next asked if the GRK2 mutations had an affect on the ability of CMPD1/2 to stabilize GRK2. Of particular interest were the L235G and L271M mutations, which had the greatest effect on inhibitor potency. The T_m for the P-loop mutations I197L and Y206S were approximately 37°C and 30°C, respectively (Figure 41B; Table 5). Thus, Y206S appears to be less stable than GRK2, yet when bound by ligand both I197L and Y206S have final T_m values similar to that of GRK2. Like the Y206S mutant, both the L235G and L271M mutations appear to be less stable with lower melting temperatures of approximately 30°C and 32°C, respectively (Figure 41C,D; Table 5).). Both mutations also show

qualitatively similar ligand induced shifts in thermal stability. Notably, the ΔT_m values for the GRK2 mutants are actually greater than the observed shifts for wild-type GRK2. However, these larger shifts are likely due to the mutations being less stable than wild type GRK2. Thus, the thermal stability data indicate that mutations around the active site of GRK2 can lead to a loss of protein stability, however, the resulting complexes have similar thermostability.

Table 5: Melting temperature changes (ΔT_m) for inhibitor bound GRK proteins. Data is representative of one to three separate experiments run in triplicate. ΔT_m is calculated by subtracting the native T_m from the inhibitor bound T_m. All values listed have units of °C.

GRK (0.1 mg/mL)	Buffer[a]	ATP (500 μM)	Balanol (20 μM)[b]	CMPD1 (100 μM)	CMPD2 (100 μM)
GRK2	36.7	5.7	19.1	16.0	12.0
-I197L[c]	37.2	--[c]	18.3	14.8	12.8
-Y206S	30.7	7.4	24.7	21.0	18.4
-L235G	29.5	7.3	23.2	20.1	17.8
-L271M	31.8	5.3	22.3	19.1	15.8
GRK1	27.2	15.4	10.1[b]	5.6	3.3
GRK5	29.4	7.8	5.5[b]	3.3	1.7

[a]The values shown for buffer alone represent the native T_m for each protein.
[b]200 μM Balanol was used for GRK1 and GRK5
[c]For GRK2-I197L the data is for n=1, with no data for ATP due to lack of additional protein.

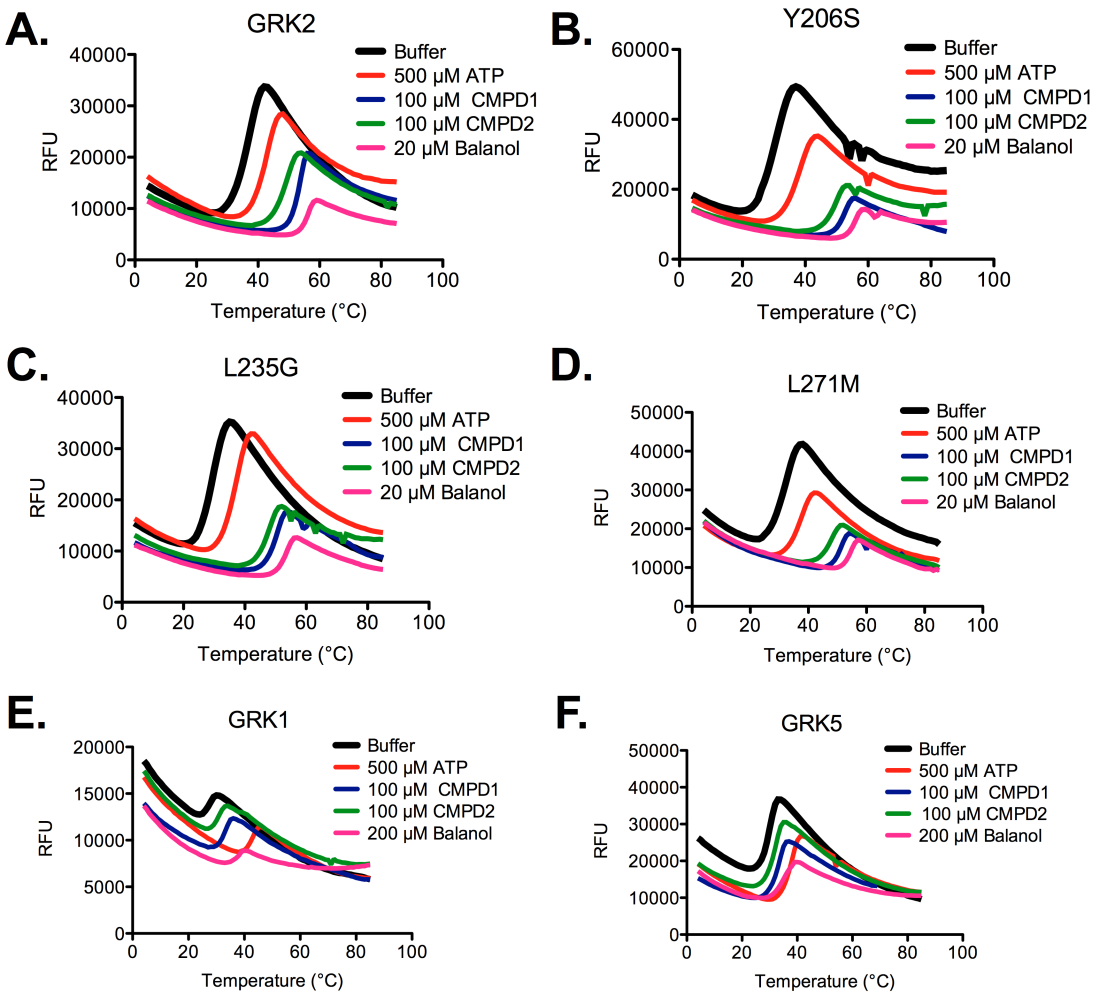

Figure 41: Thermal denaturation of GRK proteins. Representative thermal denaturation curves for **A)** GRK2, **B)** GRK2-Y206S, **C)** GRK2-L235G, **D)** GRK2-L271M, **E)** GRK1, and **F)** GRK. Thermal stability experiments were performed in triplicate, and T_m values were calculated using ThermoFluor Acquire 3.0 using the default settings of the software.

Structural Comparison against GRK1 and GRK6

So far our data suggests that individual amino acids surrounding the inhibitor-binding site do not strongly contribute to inhibitor selectivity within the GRK family. Instead it is likely that CMPDs 1/2 are stabilizing an inactive conformation of the kinase domain that is optimal for GRK2 (and probably GRK3), but not the other GRK family members. The kinase domains within the GRK family are generally well conserved with an amino acid sequence identity of ~43-49% between GRK2 and GRK1,-4,-5,-6, and -7, and ~33% between GRK2 and PKA. A common trend among the previous structures (excluding a GRK6-sangivamycin in which the kinase adopts a closed state (*194*)) is that in the absence of receptor substrate the kinase domains are in a relatively open, inactive confirmation, when compared to nucleotide-bound form of other AGC kinases. Moreover, the observed inactive states for GRK1, GRK2 and GRK6 are significantly different from each other (*186*), which would be consistent with the inhibitor data. We modeled CMPD1 and balanol in open kinase conformations to determine how well the inhibitor fits into the active site of these other GRKs, and to see if we could elucidate why balanol is less selective among GRKs.

The GRK2•CMPD1 and GRK2•Balanol structures have very similar inhibitor-binding sites (Figure 42A,B); however, one major distinction is the orientation of Asp335, which points towards the amino group linking the B and C rings of CMPD1, and towards a C ring hydroxyl group on balanol. This reorientation allows Asp335 to form favorable binding interactions with atoms that link the B

and C rings of CMPD1 and balanol. Docking of CMPD1 and balanol in the GRK1 and GRK6 structures (Figure 42C,D) show potential clashes between the C ring of CMPD1/balanol and the P-loop. For CMPD1 these clashes likely contribute to loss of affinity by forcing the residues in the P-loop to properly reorder themselves to accommodate binding. Whereas for balanol, this is a lesser problem, as balanol has substantially more hydrogen bond donors and acceptors in position to directly interact with the P-loop than CMPD1 (four versus one).

We also modeled CMPD1 into a closed conformation of GRK2 (based off the activated PKA structure) and GRK6 (from the GRK6•sangivamycin structure) to test if these compounds might also stabilize the closed kinase conformation (Figure 42E,F). The models clearly show that inhibitor binding is incompatible with the closed conformation. Overall, it seems that selectivity for CMPDs 1/2 among the GRKs is achieved by a complementary fit to the unique inactive kinase conformation of GRK2. This conformation is likely mandated by many different structural elements in GRK2, perhaps including the adjacent RH domain, which plays a scaffolding role for the kinase domain.

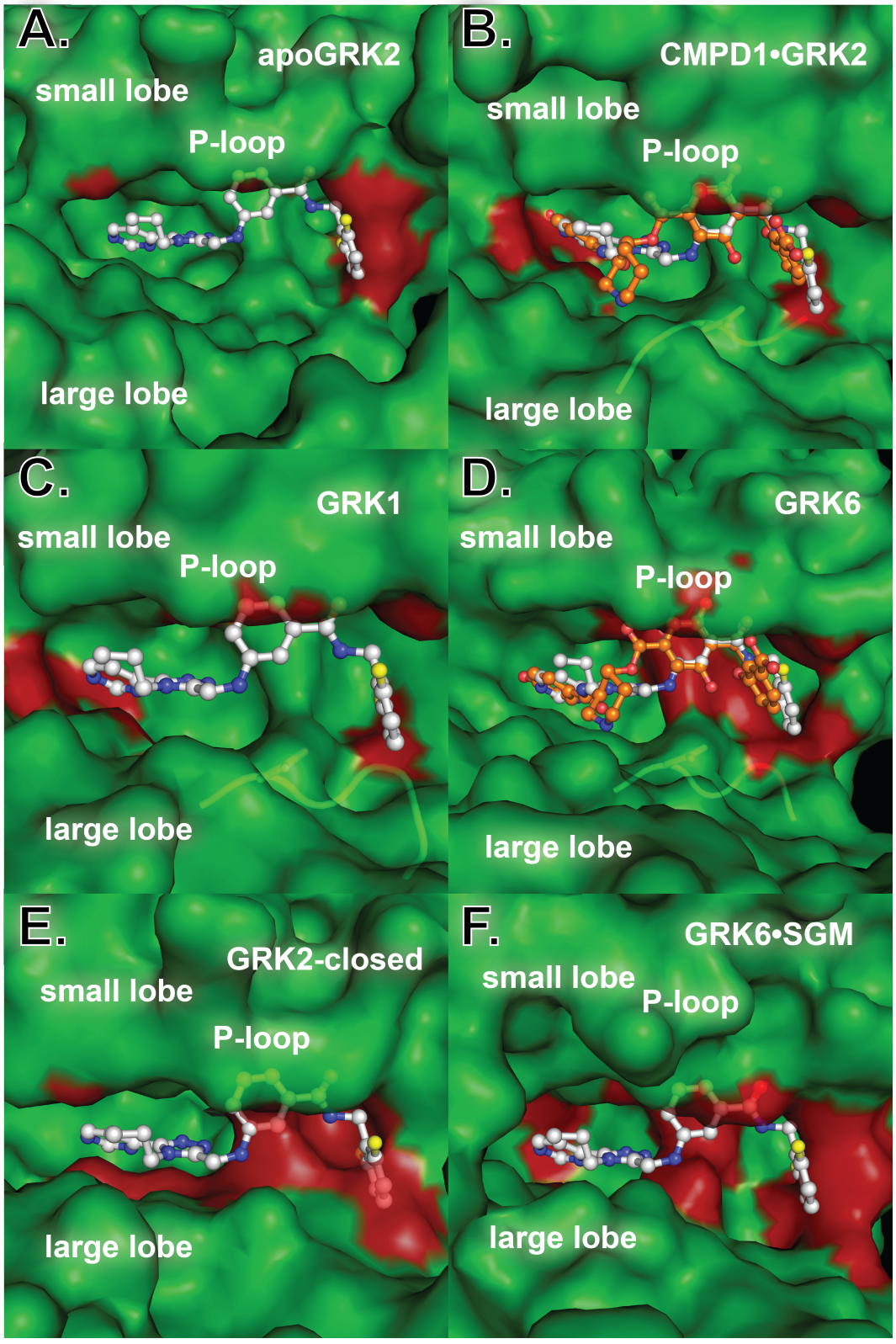
A.
apoGRK2
small lobe
P-loop
large lobe
B.
CMPD1•GRK2
small lobe
P-loop
large lobe
C.
GRK1
small lobe
P-loop
large lobe
D.
GRK6
small lobe
P-loop
large lobe
E.
GRK2-closed
small lobe
P-loop
large lobe
F.
GRK6•SGM
small lobe
P-loop
large lobe

Figure 42: Comparison of various GRK active sites docked with structurally characterized inhibitors. Surface representation of the crystal structures for **A)** apoGRK2 and **B)** GRK2·CMPD1 with balanol modeled from PDB:3KRW. CMPD1 and balanol are represented as ball and stick models. CMPD1 is shown with carbons colored white, nitrogens blue, oxygens red, and fluorines yellow. Balanol is shown with carbons colored orange. CMPD1 and balanol modeled into the **C)** GRK1•ATP (3C4W) and **D)** GRK6•AMPPnP (2ACX) structures. CMPD1 docked with **E)** GRK2 and **F)** GRK6 kinase domains in closed kinase conformations. All structures were superimposed using the small lobe of the GRK2·CMPD1 structure. The red surface coloring represents atoms that are with 3.5 Å of CMPD1 are not involved in obvious hydrogen bond interactions. The closed kinase conformation for GRK2 was modeled after the activated structure of PKA (1L3R), and the GRK6 closed conformation is that of the GRK6·sangivamycin structure (3NYN).

CONCLUSIONS

Crystal structures of protein kinases have provided valuable insights for the rational design of selective kinase inhibitors. Numerous mechanisms for achieving inhibitor selectivity have been discovered including the stabilization of a unique inactive conformation (Gleevec) or targeting a less conserved hydrophobic pocket (such as the one guarded by the “gatekeeper” residue). Our crystal structures of GRK2 bound to CMPD1 and CMPD2 reveal that these inhibitors bind in the active site of GRK2 in its open conformation, much like the

non-selective AGC kinase inhibitor balanol. All of these inhibitors induce a similar slight closure of the kinase domain. The binding of balanol to GRK2 induces a 4.0° domain closure, whereas CMPD1 and 2 induce 3.6° and 2.4° closures, respectively. Interestingly, the degree of domain closure correlates to the potencies of the inhibitors, suggesting that the affinity is derived from stabilizing a binding-mode that is related to the degree of domain closure. Furthermore, selectivity among the GRK family is likely due to different degrees of domain closure in the inactive, open state of the various GRKs. It would certainly being interesting to test fragments of CMPDs 1/2 in both phosphorylation assays and crystallization trials to determine if a particular pharmacophore could be developed that could be utilized, with additional structure activity relationships, to develop inhibitors with selectivity more towards GRK4 subfamilies.

Chapter 5
Development of a Novel Aptamer Displacement Assay Targeting the Inactive Conformation of GRK2

BACKGROUND AND PROJECT GOALS

The G protein-Coupled Receptor Kinase (GRK) Family.

GPCR desensitization is initiated by G protein-coupled receptor kinases (GRKs), which catalyze the phosphorylation of serine and threonine residues in the cytoplasmic tails and loops of most, if not all activated GPCRs (*15, 195, 196*). These phosphorylated receptors are then bound by molecules of arrestin, which uncouple the GPCRs from G proteins (*197-199*), target the receptors to clathrin-coated pits for endocytosis (*15, 200*), and serve as adaptors for other signaling pathways such as those of the MAP kinases (*201, 202*). For example, in visual phototransduction, the uncoupling of rhodopsin occurs within 80 ms such that only ~20 G proteins become activated after a single photon is absorbed (*203*). GRKs are found in all metazoans and classified into three subfamilies based on their gene structure and homology. The GRK1 subfamily is vertebrate specific and consists of GRK1 (rhodopsin kinase) and 7, which are expressed in the rod and cone cells of the retina. The GRK2 subfamily, consisting of GRK2 and GRK3, are ubiquitously expressed. The GRK4 subfamily consists of GRK4, 5 and 6. GRK5 and 6 are ubiquitously expressed, while GRK4 is found primarily in

testes and kidneys. All metazoans contain at least one member representing both the GRK2 and GRK4 subfamilies.

The central, catalytic domain of GRKs is a serine/threonine kinase domain that is ~32% identical in sequence to the catalytic subunit of protein kinase A (PKA) and is a member of the PKA, PKG and PKC (AGC) family of kinases (*204, 205*). The kinase domain consists of two lobes, termed the small (or N) and large (or C) lobes. ATP binds at the interface of these lobes, adjacent to a shallow canyon formed primarily by the large lobe where polypeptide substrates bind. The ATP binding site is highly conserved among all protein kinases, and is the binding site for all reported inhibitors of GRKs.

Regulatory Role for GRK2 in the Cardiovascular System.

There is ample evidence that GRK2 regulates cardiac β-adrenergic receptors (βARs). Activation of cardiac βARs causes the opening of calcium channels, which strengthens and increases the rate of contractions. Removal of GRK2 phosphorylation sites at the carboxyl terminus of the receptor abrogates desensitization (*206*), whereas co-expression of β_2AR with wild-type GRK2 (*207*), but not a kinase-deficient mutant (K220R) of GRK2, enhances desensitization (*208*). Furthermore, overexpression of GRK2 in cardiac myocytes leads to attenuated catecholamine-induced βAR signaling, whereas overexpression of the C-terminal domain of GRK2 (GRK2ct), which inhibits GRK2 through a dominant negative mechanism, has the opposite phenotype (*123*).

During congestive heart failure (CHF), uncoupling of βARs from downstream effectors is observed at early stages, coinciding with increased activity and expression of GRK2. This event precedes modifications in the expression and maintenance of β_1ARs, G proteins or adenylyl cyclases (*209-213*). Furthermore, cardiac-restricted expression of GRK2ct in mouse models of cardiomyopathy reduces heart failure in these animals (*214, 215*). For these reasons, GRK2 is considered an important drug target for the treatment of CHF. Cardiac βARs are not the only important targets of GRK2. A class of drugs known as β-blockers (βAR antagonists) is among the most widely prescribed to treat heart disease. The fact that β-blockers are protective, while overexpression of GRK2, an endogenous βAR inhibitor, is maladaptive, suggests that GRK2 also broadly regulates the activity of other important receptor groups in the heart, including α-adrenergic and angiotensin receptors. GRK2 may also be responsible for modulating additional pathways that ultimately lead to cardiac failure (*216*), such as stimulating the release of excess catecholamines from adrenal cells (*217, 218*), which is detrimental to the failing heart.

Known Inhibitors of GRK2

The Uninteresting Inhibitors of GRK2

Benovic *et al.* reported the first inhibitors of GRK2 in 1989 (*219, 220*). These inhibitors were polyanions and included compounds such as heparin, dextran sulphate, suramin, and even Zn^{2+}, which for obvious reasons represent poor drug

leads. Numerous non-selective pan-kinase inhibitors are known to inhibit GRK2, such as staurosporine, tamoxifen, and sangivamycin with IC_{50}'s ranging from 20 μM to 250 μM (*221*).. Moderately potent peptide inhibitors of GRKs have also been described, but these have poor solution properties, low membrane permeability, and little selectivity among GRKs (*222, 223*).

Balanol

Balanol is very potent natural product kinase inhibitor that is isolated from the fungus *Verticillium balanoides (224).* Balanol inhibits GRK2 with the greatest potency (K_i ~2 nM), but is a relatively non-selective inhibitor of AGC kinases (*175*). Balanol has been the subject of extensive crystallographic studies and structure activity relationships (SAR) to develop selective inhibitors between PKA and PKC (*177, 190, 225, 226*).

The Takeda Compounds

In 2007, several small molecule inhibitors were described by Takeda Pharmaceuticals that are both potent and selective against GRK2 (*176*). According to the patent, these compounds are cell permeable, and when applied to isolated perfused heart samples increase left ventricular pressure. Further experiments in rats revealed that these compounds acutely improve contractive force and have little effect on heart rate. These compounds thus represent the first cardiotonic drug that consists of a GRK inhibitor. However, these compounds are believed to suffer from poor drug properties and were apparently

dropped from further development. We have solved the crystal structure of two of these compounds bound in the active site of GRK2, and their structural basis for selectivity primarily appears to be the stabilization of a distinct inactive kinase conformation (see Chapter 4).

The C13 RNA Aptamer

Aptamers are oligonucleotides that are selectively amplified from a pool of randomized sequences based on their ability to bind a specific target. The resulting affinities and specificities can be similar to monoclonal antibodies (*227*). Using this approach, a 51-nucleotide RNA aptamer (C13) that inhibits GRK2 kinase activity with a K_d of 100 nM was reported in 2008 (*228*). The C13 aptamer showed remarkable specificity for GRK2, exhibiting a ~20-fold higher IC_{50} for GRK5 in activity-based assays, and does not appreciably inhibit other closely related kinases. Our lab has recently solved a 3.5 Å crystal structure of a slightly modified aptamer bound to the kinase domain of GRK2 (V. Tesmer, personal communication), which adopts a conformation similar to that seen in both the balanol and Takeda compound complexes with GRK2 (see Chapter 4). However, the aptamer also appears to induce rearrangements in the large lobe of the kinase domain.

A New Approach to Identify Selective Inhibitors of GRK2.

Traditional kinase screening methods are mainly focused on enzyme activity assays. Because the active site of kinases are typically well conserved this

creates an assay bias for discovering inhibitors that generally lack selectivity (*229, 230*). As Noble *et al.* (*170*) so eloquently paraphrased from *Anna Karenina*, “all active kinases are alike, but an inactive kinase is inactive after its own fashion.” Thus, targeting an inactive kinase conformation represents a greater potential for achieving drug selectivity. Indeed, the crystal structure of Gleevec bound to the Abl kinase domain revealed that Gleevec locked the kinase domain into an inactive conformation that even closely related kinases were unable to adopt (*231, 232*). Our crystal structure of the C13 aptamer bound to GRK2 suggests that the aptamer also stabilizes a unique inactive conformation. Small molecules have been indentified via aptamer displacement assays that exhibit similar properties as the bound aptamer (*232*). We hypothesized that small molecules that can displace the binding of the C13 aptamer could likewise be selective and lead to a new generation of useful GRK2 inhibitors.

Project Goals

The initial goal of this project is to discover a small set of small molecule probes that can later be developed into a more potent, selective, and drug-like inhibitor of GRK2. We anticipate discovering compounds that fall into one of four different classes or types (*189, 230*). Type I inhibitors bind in the active site and occupy the ATP binding site. Type I inhibitors are generally less selective, but inhibitors with a potency of 100 nM or better could still be used as SAR leads. Type II inhibitors are similar in structure/function to the Takeda compounds and span both the active site and an additional hydrophobic pocket outside of the active

site. Type II inhibitors tend to display greater selectivity profiles and are of immediate interest if they also display good potency. Type III inhibitors do not bind in the active, and are generally less potent than type I/II inhibitors. However, like type II inhibitors they tend to have superior selectivity profiles. In our case, we also define Type IV inhibitors (also referred to as class 2 compounds) which bind to other aptamer binding sites that are not important for receptor phosphorylation. Assuming these compounds specifically inhibit the aptamer-GRK2 interaction, they could represent novel leads with additional SAR and crystallographic studies. We are primarily interested in discovering type II/III inhibitors, and we believe the RNA aptamer displacement assay will serve as a novel tool to identify such inhibitors. Overall, the identification of new GRK2 inhibitors, coupled with structure activity relationships and crystal structures of there compounds in complex with GRK2 will enable a powerful rational drug design process that will hopefully lead to the generation of a new therapeutic for the treatment of heart disease.

METHODS

Purification of GRK2

Bovine and human GRK2-S670A was purified as described before (*100*). The S670A mutation removes a MAP kinase phosphorylation site, which has no influence on in vitro kinase activity.

Preparation of Screening Reagents

RNA Aptamer

The original 51-nucleotide RNA aptamer (C13.51) was truncated at the stem to create a smaller 28-nucleotide construct (C13.28) with the following RNA sequence 5'-GGCAGACCAUACGGGAGAGAAACUUGCC-3'. The RNA was fluorescently labeled on the 3' end with 6-carboxyfluorescein (FAM) and is referred to as C13.28-FAM. An additional RNA construct consisting of 5' biotin label on C13.28-FAM was used as a counter-screen probe and is referred to as biotin-C13.28-FAM. All RNA reagents were synthesized and purchased from Integrated DNA Technologies.

FCPIA and High-Through Screening.

Biotinylated GRK2 (bGRK2) was synthesized as described in Chapter 3. FCPIA and HTS were performed as previously described for $G\alpha_q$-GRK2 with modifications. In brief, bGRK2 (5 nM, final concentration) was immobilized onto streptavidin beads and resuspended in assay buffer consisting of 20 mM HEPES pH=7.0, 50 mM NaCl, 5 mM $MgCl_2$, 1 mM CHAPS, 0.2% lubrol, and 2 mM DTT. Test compounds were spotted in 0.2 μL of DMSO into individual wells of 384-well plate that contained 10 μL of assay buffer in each well. Subsequently, 5 μL of bead bound bGRK2 was added to each well, except for columns 23/24, which contained blank beads and served as the positive control. Test compounds were allowed to incubate for at least 15 minutes with bGRK2. We then added 5 μL of C13.28-FAM to each well at final concentration of 5 nM. Minor modifications

were made to the HTS protocol for screening against the Chembridge 100k collection and the MLSCN collection at the University of New Mexico, including the use of 10 mM NaCl instead of 50 mM NaCl in the assay buffer. Streptavidin beads were also labeled with 25-50 nM bGRK2 (final concentration), and the final concentration of C13.28-FAM was 2.0 nM. For the MLSCN screen 100 nM unlabeled aptamer was used as the positive control.

Phosphorylation Assays

Inhibition of phosphorylation of bovine rod outer segments (bROS; rhodopsin) by GRK2 was performed as described in Chapter 4 with changes to the ATP concentration used. In brief, reactions were carried out in a 96-well PCR plate with 2.0 μM bROS, 25 nM GRK2, varying concentrations of compounds, 3-25 μM ATP+[γ^{32}P-ATP], and quenched at a time point of ~20 min. Phosphorylation of rhodopsin was analyzed by SDS-PAGE and phosphor-imaging.

RESULTS

FCPIA Measurements of the Aptamer-GRK2 Interaction

Initial measurements of aptamer binding to GRK2 were done via fluorescence polarization (FP) using a fluorescently labeled 28-nucleotide version of the C13 aptamer (C13.28-FAM), which has a K_d of 2.0 nM (Figure 43A). However, the signal-to-noise ratio (S/N) using FP was less than 2, which proved to not be amenable for HTS. Thus, we optimized FCPIA for use with the aptamer, with

only minor modifications to our original FCPIA protocol. Using FCPIA, we measured a K_d identical to that determined by FP (Figure 43B). More importantly, we observed a dramatic increase in the S/N (>10), which allowed us to use low concentrations of aptamer (2–5 nM) and produce Z-factors that were consistently over 0.8.

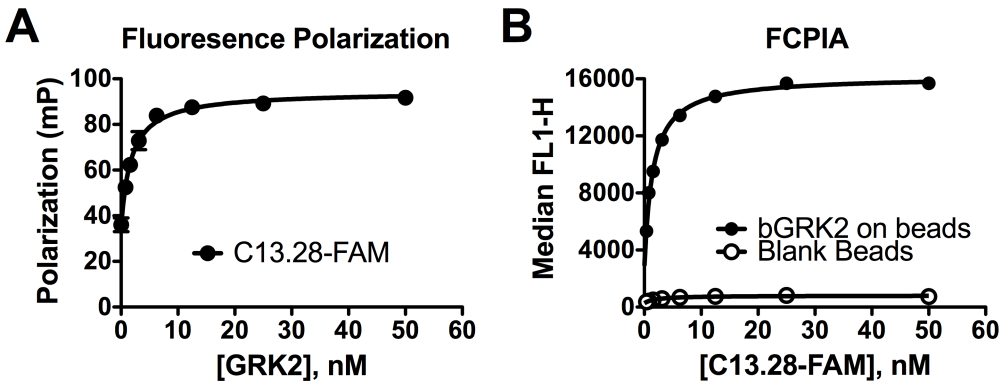

Figure 43: Binding of C13.28-FAM to GRK2. A) The binding of RNA aptamer to GRK2 as measured by FP **B)** and FCPIA. Both techniques give a K_d value of 2.0 nM. The S/N ratio (at the K_d) for FP and FCPIA is <2 and >10, respectively. The data shown is mean ± SEM values, run in duplicate and representative of n≥3 experiments.

The intent of our high-throughput screen is to discover small molecule inhibitors that have selectivity profiles similar to the aptamer. The Takeda inhibitors (CMPD 1 and CMPD 2) represent good examples of compounds we would like to discover. We tested both of these compounds, along with balanol, in dose-response titrations against C13.28-GRK2 to ensure that our assay is working as

intended. Our previous results from phosphorylation assays showed that in terms of potency balanol > CMPD 1 > CMPD 2. These results qualitatively matched the results from dose-response titrations against the aptamer (Figure 44). Therefore, our assay is functional in indentifying selective inhibitors of GRK2 activity. Althoughj, this data also indicates that we will not be able to directly determine inhibitor selectivity using this assay.

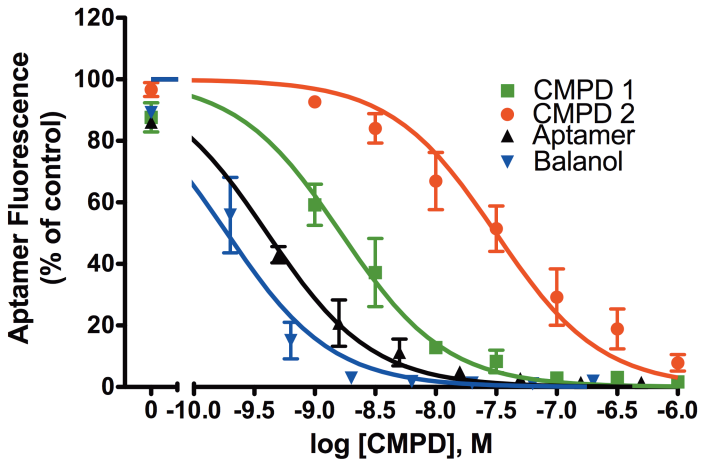

Figure 44: Inhibition of aptamer binding by known GRK2 inhibitors. Dose-response titrations of CMPD 1, CMPD 2, balanol, and unlabeled aptamer against 2.0 nM C13.28-FAM. The IC_{50} values range from 30 nM for CMPD 2 to 0.2 nM for balanol (n=4, in duplicate).

Primary Screening Results for Aptamer-GRK2

Our initial high-throughput screen tested ~47,000 compounds for activity against C13.28-GRK2. The Z-factors over the course of the screen were between 0.7 and 0.9 per plate. We triaged the data in collaboration with the CCG and

MCCSL using hit criteria similar to the $G\alpha_q$-GRK2 screen. Overall, the triage resulted in 1,153 compounds being selected for follow-up activity. We tested the primary screen hits in a confirmation screen that consisted of testing each compound at 10 μM, in triplicate, and were able to confirm activity for 110 compounds. We then proceeded to test them for activity in follow-up dose-response titrations and phosphorylation assays.

Elimination of False Positive Primary Screen Hits

We tested our 110 confirmed primary screen hits in dose-response titrations with a concentration range of 30 nM to 100 μM. Out of the 110 compounds, 86 compounds tested positive for activity with IC_{50} values ranging from 2 nM to 5 mM. We also tested all 110 compounds in a single point phosphorylation assay using 10 μM bROS, 25 nM GRK2, 25 μM ATP, and a compound dose of 50 μM. Data was normalized to controls consisting of 1% DMSO and 10 μM balanol. Of the 86 compounds tested, 29 compounds inhibited GRK2 by more than 15%. We subsequently ranked the 29 compounds by their IC_{50} value, percent inhibition, and vendor availability. Twenty compounds were purchased and came from either the Maybridge or ChemDiv collections.

Specificity of CCG Compounds on Inhibiting C13.28-FAM/bGRK2.

Ordered compounds were tested for activity in dose-response titrations against C13.28-FAM/bGRK2 (Figure 45A), $G\alpha_{13}$-LARG (data not shown), and biotin-C13.28-FAM (Figure 45B). Compounds that lacked activity against aptamer-

GRK2, or displayed activity against either $G\alpha_{13}$-LARG or biotin-C13.28-FAM were eliminated from further consideration. These criteria resulted in 7 compounds that appear to specifically inhibit formation of the aptamer-GRK2 complex (Figure 46). Unfortunately, all of our nanomolar inhibitors that made it to this point were also active in our counter-screen assay ($G\alpha_{13}$-LARG or biotin-C13.28-FAM).

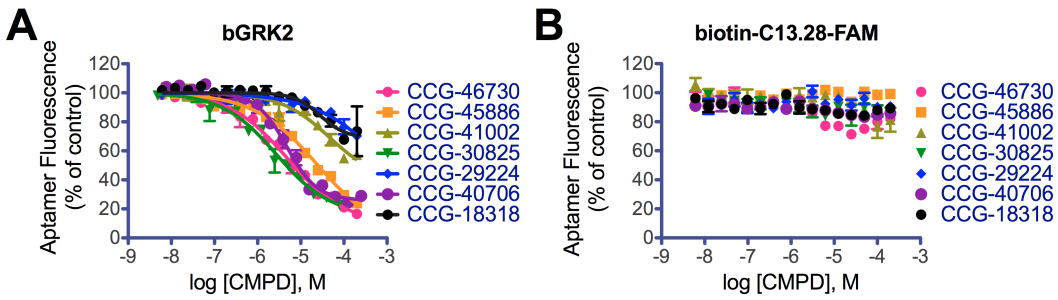

Figure 45: CCG compounds specifically active against aptamer-GRK2. A) Dose-response titrations against 2 nM C13.28-FAM bound to bGRK2. **B)** Fluorescent counter-screen using biotin-C13.28-FAM immobilized on beads. Data is normalized to the positive (blank beads) controls and negative controls (DMSO), and fit to a four-parameter dose-response curve using Prism 5.0c. IC_{50} values and hill-slopes are reported in **Table 6.** Data shown is mean ± SEM values and is representative of n≥3 experiments run in duplicate.

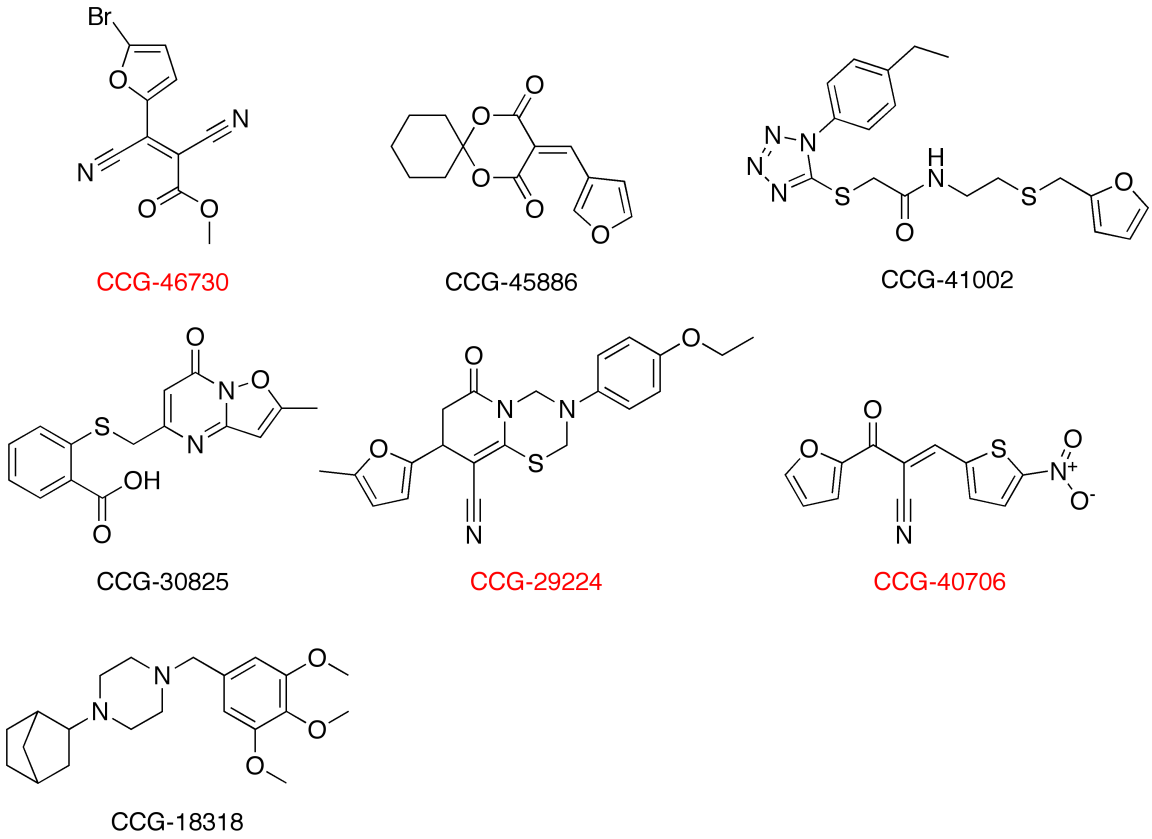

Figure 46: Chemical structures of active CCG compounds from the aptamer-GRK2 screen. Compounds labeled in red are listed as red flags in the Mscreen database, indicating that they contain highly reactive or toxic motifs that may lead to aberrant results.

Initial Characterization of the Inhibitory Effect of Seven CCG Compounds. Three compounds (CCG# 46730, 45886, and 41002) were tested in full dose-response titrations for their ability to inhibit the phosphorylation of rhodopsin (bROS) by GRK2 (Figure 47). Only CCG-46730 displayed significant activity with an IC_{50} value of 21 μM (n=3). CCG-41002 only inhibited GRK2 at high concentrations (500 μM) at which compound solubility and aggregation are more

likely to be the basis for inhibition (*233*). It was initially surprising that CCG-45886 did not inhibit GRK2 activity. However, the compound was also found as active in a DNA-binding screen run in the CCG indicating that the compound is likely to be a DNA/RNA intercalater. We recently tested four additional CCG compounds in a phosphorylation assay against both GRK2 and GRK1 (Table 6). Although the results are still preliminary, CCG-30825 appears to inhibit both GRK2 and GRK1 with an IC_{50} value under 25 μM. The other compounds could possibly be binding to other aptamer binding sites that are not important for receptor phosphorylation, and will be tested in an intercalator displacement to determine if they bind to the RNA aptamer.

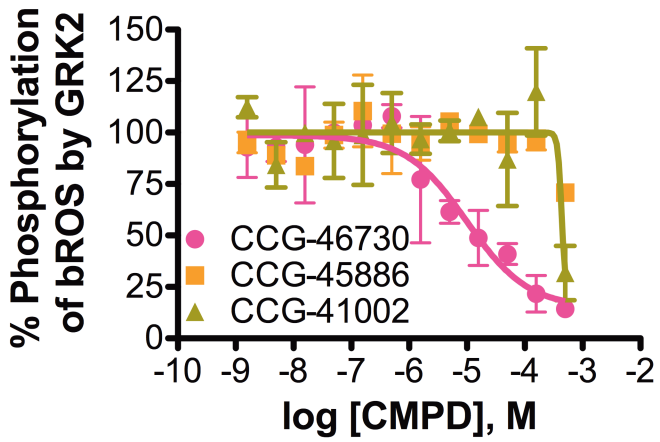

Figure 47: Inhibition of GRK2 activity by CCG-46730. Phosphorylation assay was carried out with 2 μM bROS, 25 nM GRK2, 3 μM ATP with a 20 minute time point. The IC_{50} value for CCG-46730 is ~ 21 μM (n=3). The IC_{50} for CCG-41002 is well over 200 μM is likely a non-specific inhibitor. The results shown are mean ± SEM values for one experiment run in duplicate.

Table 6. Summary of results for CCG compounds that are specifically active against aptamer-GRK2. NA, not active; ID, indeterminate.

Compound	C13.28-GRK2[A]		GRK2 Activity[B]
CCG#	IC_{50} (μM)	Hillslope	IC_{50} (μM)
46730	4.9	-0.7	21
45886	25	-0.6	NA
41002	47	-0.8	> 150 uM
30825	3.4	-0.7	< 25[C]
29224	>100	-0.5	> 25[C]
40706	3.8	-1.2	ID[C]
18318	28	-1.4	NA[C]

[A]Competition FCPIA using 2.0 nM C13.28-FAM. [B]Inhibition of bROS phosphorylation by GRK2. [C]Compounds were tested at concentrations of 25 μM and 250 μM (n=1) against both GRK2 and GRK1.

Additional HTS Campaigns Against Aptamer-GRK2.

We have recently performed two additional screens against the Aptamer-GRK2 interaction. The first was ~320k compound screen run in collaboration with the MLSCN at The University of New Mexico. The screen resulted in ~1,700 hits (0.6% hit rate) using three standard deviations as the cut-off. These compounds are currently being tested in dose-response titrations. We have also recently finished screening the 100k ChemDiv collection at the CCG, and are set to test 412 compounds in dose-response titrations (0.4% hit rate after confirmation with a 20% cutoff).

DISCUSSION

It is estimated that over 25% of all pharmaceutical drug targets are protein kinases making them the second largest class of drug targets behind GPCRs (*234*). Conventional kinase assays rely on enzymatic reactions were inhibition of substrate phosphorylation is used a means for target identification. This type of assay has a bias for indentifying what is described as type I inhibitors (*229, 230*), which bind to the ATP binding site and usually target the active state of the kinase. Selectivity for type I inhibitors is usually low due to the high conservation of amino acids in the active site. Type II kinase inhibitors bind in the ATP binding site, but also extend into a hydrophobic pocket that is created by the inactive conformation of the kinase (DFG-out). Lower affinity type III inhibitors have also been identified that bind only in the allosteric site (*170, 171, 189, 229, 230, 235*). Structural analysis of type II inhibitors bound to their targets have revealed three key interactions: 1) a hydrogen bond to the conserved glutamic acid in the αC helix, 2) a hydrogen bond to the backbone amide of the aspartic acid in the DFG motif, and 3) a hydrophobic moiety that forms van der Waals interactions with the allosteric site (*189*). Our crystal structures of the Takeda compounds (CMPDs 1/2) bound to GRK2 identified these compounds as type II inhibitors. These inhibitors display exquisite selectivity towards GRK2, and replicated results from previous studies showing that inhibition of GRK2 increases contractility of the heart (*176*). Overall, the Takeda inhibitors serve as very important proof-of-concept that a GRK2 inhibitor is a useful cardiotonic drug, however, the inhibitors

appear to lack properties that will turn it into a useful drug because the patent seems to be dropped.

To address the needs for a new GRK2 inhibitor, we developed a kinase assay using FCPIA that utilizes a new discovered RNA aptamer that selectivity inhibits GRK2 in mechanism that appears analogous to the Takeda compounds. We believe that displacement of the RNA aptamer by small molecules could lead to the discovery of a series of novel GRK2 selective inhibitors with type II/III properties (not excluding the rare possibility of finding a selective type I inhibitor). We showed in competition assays that known type I (Staurosporine, data not shown) and type II inhibitors are capable of displacing the aptamer with IC_{50} values similar to those derived from phosphorylation assays. Thus, displacement of the aptamer is valid approach for the detection of kinase inhibitors. The FCPIA format is well documented for its HTS performance as described in Chapter 3 and elsewhere (*102, 151, 154*). The resulting aptamer displacement assay produces an HTS method that does not rely on an enzymatically active kinase, and will lead to an enrichment of hits that bind to the inactive kinase conformation, thereby increasing our odds of finding a selective inhibitor.

To date we have screened almost 500,000 compounds against aptamer-GRK2 with observed Z-factors of ~0.9 demonstrating that our assay is well engineered for HTS. However, as seen with the $G\alpha_q$-GRK2 screen our HTS campaign against aptamer-GRK2 using FCPIA is certainly not without problems, most

notably a high false positive hit rate. Our initial ~47,000 compound screen resulted in 1,153 primary screen hits, although it should be noted that defining a hit rate at this step is somewhat trivial as we adjusted our triage criteria to produce as many hits as we felt comfortable testing (i.e. 1,200). Out of the 1,153 primary screen hits we had 110 compounds reconfirm activity with 86 having activity in subsequent dose-response titrations. Out of the 86 compounds only 29 had activity in phosphorylation assays (with a modest cut-off of 15%), and upon reordering our 20 best hits, only seven compounds specifically inhibit the aptamer-GRK2 interaction via FCPIA. We are currently following up the activity of these seven compounds in phosphorylation assays against GRK2 and GRK1. Currently, CCG-46730 and CCG-30825 represent our best leads with IC_{50} values of less than 25 μM for inhibition of GRK2. The potency of these compounds is only modest, but they could serve as the starting point for future selectivity assays, structure activity relationships, and crystallization efforts that could lead to a more potent inhibitor. Immediate future directions will be primarily focused on increasing the workflow of our secondary assays and development of a cell-based tertiary assay.

Overall, the combination of an aptamer displacement assay with FCPIA provides a simple and reliable approach that can be used to screen for selective small molecule inhibitors of GRK2 that stabilize the inactive kinase conformation. To our knowledge the FCPIA aptamer displacement assay is one of only two

methods (*230*) currently available that are capable of discovering type II/III inhibitors in a HTS format.

FUTURE DIRECTIONS

The aptamer-GRK2 project is currently at a stage were we are awaiting the results for ~2,100 compounds being testing in dose-response titrations against both C13.28-FAM/bGRK2 and biotin-C13.28-FAM (as a counterscreen). Based on previous results, we would expect around 10% of the compounds to follow-up with specific activity. The obvious secondary assay for testing the activity of subsequent hits is by directly testing them for their ability to inhibit the phosphorylation of a receptor target (bROS) by GRK2. However, our current technique is rather tedious (as it is a radiometric assay) when applied to a high-throughput scale and is limited to testing 4 compounds per day when using full dose-response curve in duplicate. We plan to optimize the ADP-Glo Kinase Assay (Promega) for use with GRK2 and GRK1. The ADP-Glo assay is currently in use at the CCG is very amenable to HTS in a 384-well format. Furthermore, the assay is already available for over 48 different kinases and will thus be very useful for kinase profiling. With this assay we could expect to easily test up to 20 compounds per day against 5 different kinases with full dose-response titrations.

We also intend to develop an *in vivo* assay to test the ability of future inhibitors to inhibit GRK2 in cells. Kenski *et al.* utilized a fluorescence flow-cytometry assay that measures the internalization of an epitope tagged μ-opioid receptor in

HEK293 cells that overexpress GRK2 (*236*). They show in a very specific manner that inhibition of GRK2 leads to a significant decrease in the percent internalization in response to treatment of cells with morphine. Given that the primary strength of our collaborators in flow cytometry, this assay should prove quite feasible.

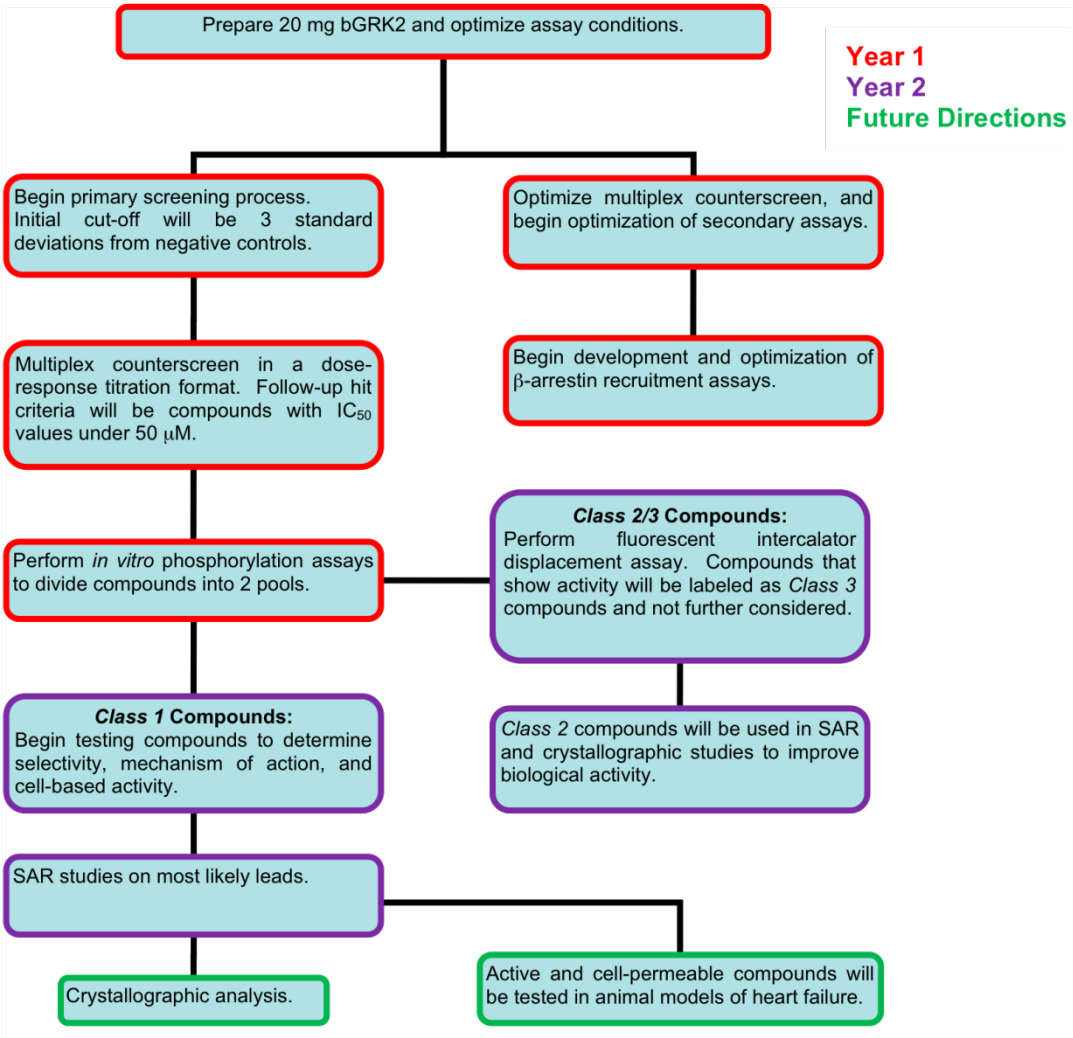

Figure 48: A minimal path flow chart for aptamer-GRK2 project. Class 1 compounds represent compounds that are active in phosphorylation assays, will then be tested for their ability to bind in the nucleotide binding pocket using an ADP displacement FP assay. Compounds that bind in the nucleotide binding

pocket will be termed subclass 1 hits and have a lower priority over compounds that bind outside the active site (subclass 2). Compounds that do not show activity in phosphorylation assays will be tested in an intercalator displacement assay to test for binding against the aptamer. Compounds with activity in the intercalator assay will be dropped (class 3), and non-active compounds (class 2) will undergo SAR to try and improve biological activity.

Chapter 6
Conclusions and Future Studies

Transmembrane signaling through $G\alpha_q$-coupled receptors is linked to physiological processes such as cardiovascular development, platelet activation, and smooth muscle function. The classic activity of $G\alpha_q$ is activation of the inositol lipid signaling pathway through PLCβ. However, $G\alpha_q$ has also been shown to interact with various downstream signaling proteins including RGS proteins (RGS2 and RGS4), p63RhoGEF, and GRK2. There is ample evidence linking RGS2, RGS4, p63RhoGEF, and GRK2 to distinct signaling roles in the cardiovasculature. For example, RGS2 knockout mice have hypertensive phenotypes, whereas p63RhoGEF has been implicated in actin cytoskeleton reorganization in cardiomyocytes. The $G\alpha_q$-GRK2 interaction is of particular interest in that GRK2 binds $G\alpha_q$ like an effector protein, suggesting that GRK2 can initiate its own signaling cascade. Furthermore, GRK2 is strongly linked to heart failure and is considered a major pharmaceutical target.

Overall, this thesis can be divided into two sections, with GRK2 playing a major role in each. The first half (Chapters 2 and 3) is an investigation of the functional importance of the protein-protein interactions involved in the $G\alpha_q$ signaling pathway, with emphasis on the $G\alpha_q$-GRK2 interaction. The second half (Chapters 4 and 5) is aimed at drug discovery towards GRK2 with an emphasis

on determining the mechanism of selectivity for a family of GRK2 inhibitors, and development of a novel assay for screening for new inhibitors of GRK2.

Protein-Protein Interactions of the $G\alpha_q$ Signaling Pathway

The $G\alpha_q$ subunit is capable of forming numerous protein interactions with targets including: the $G\beta\gamma$ subunit, GPCRs, RGS proteins, PLCβ, p63RhoGEF, and GRK2. Each of these interactions is important in controlling the diverse range physiological responses mediated by the activity of $G\alpha_q$. In Chapter 2, we have shown that ternary complexes can form between $G\alpha_q$, RGS2/4, and either GRK2 or p63RhoGEF. The formation of these complexes exhibits significant allostery, similar to the behavior observed in a ternary complex between $G\alpha_t$, PDEγ, and RGS9. The allosteric modulation derived from the formation of these ternary complexes provides a mechanism where the level of signaling through the $G\alpha$ subunit is more finely tuned.

We have also shown that the $G\alpha_q$ interaction with GRK2 and p63RhoGEF is allosterically modulated by RGS2 and RGS4. This data corroborates the hypothesis that GRK2 is a *bona fide* effector of $G\alpha_q$. From this, we hypothesize that RGS proteins can regulate receptor phosphorylation mediated by GRK2. This type of novel regulation is interesting in that upregulation of RGS proteins would discourage GPCR uncoupling and downregulation, and at the same time suppress $G\alpha_q$ signaling. Thus, RGS accelerated GTP hydrolysis would prevent

$G\alpha_q$ signaling while preserving receptor number and function by inhibiting GRK2 function.

In addition to the phosphorylation of activated GPCRs, GRK2 has been shown to phosphorylate IRS-1, p38 MAP kinase, and ezrin in response to activation of $G\alpha_q$-coupled receptors. To date, no signaling pathway has been explicitly linked to $G\alpha_q$ directly activating GRK2. Indeed, both $G\alpha_q$ and GRK2 are strongly implicated in the development of cardiac disease and hypertension. However, it is unclear if the roles of $G\alpha_q$ and GRK2 in cardiovascular pathophysiology are linked. For example, inhibition of GRK2 produces a beneficial effect towards the treatment of heart failure. This beneficial effect is quite paradoxical when considering the protective effect of interrupting β-AR signaling with β-AR antagonists, suggesting that regulation of other receptors in the heart, such as the $G\alpha_q$-coupled α-adrenergic and angiotension receptors, by GRK2 could play a role heart disease. Thus, our goal of Chapter 3 was to run a high-throughput screen against formation of the $G\alpha_q$-GRK2 complex to try and develop a small molecule inhibitor against the PPI. Overall, we were largely unsuccessful in finding a specific small molecule inhibitor of the $G\alpha_q$-GRK2 interaction, further highlighting the extreme difficulties associated with inhibiting PPIs with small molecule inhibitors. Whereas further studies could be aimed at screening larger chemical libraries or perhaps libraries better suited towards inhibiting PPIs, alternative strategies for inhibiting PPIs could prove more fruitful such as the design of miniature proteins or functional oligonucleotides.

Nevertheless, investigation of the functional importance of PPIs involved in GPCR signaling pathways remains an exciting area of research, and it will be critical to gaining a complete understanding of the complex physiology that is often associated with these pathways. Furthermore, given the regulatory impact of many of these interactions, the development of small molecule inhibitors that defeat these interactions could lead to unique and more selective types of therapeutic intervention.

The Inactive Kinase Conformation of GRK2

Crystal structures of protein kinases have provided valuable insight into the rational design of selective kinase inhibitors. In Chapter 4, we co-crystallized two selective kinase inhibitors bound to GRK2. Our crystal structures reveal that these inhibitors stabilize distinct inactive conformations of the GRK2 kinase domain that are not accessible to other GRK subfamilies. These unique inactive states are suggested by prior crystal structures of GRK1 and GRK6, and likely result from sequence differences within the kinase domain as well as in the adjacent RH domain, which plays a scaffolding role in these enzymes. Based on our crystal structures and homology modeling we identified five amino acids surrounding the inhibitor-binding site that we hypothesized could also contribute to inhibitor selectivity. Our biochemical results, however, indicate that these individual amino acids are not major determinants for inhibitor selectivity among GRK family members. This is in direct contrast to previous studies, in other AGC

kinases, that suggest that individual residues of the binding site can play major roles in dictating selectivity of kinase inhibitor interactions (*192*). Future studies aimed at determining crystal structures across the GRK subfamily with different ligand complexes and crystallization conditions will provide a better molecular understanding of kinase flexibility and provide the molecular basis for how selectivity is achieved among the GRK subfamily.

Recently, an RNA aptamer has been discovered that is capable of selectively inhibiting GRK2 with nanomolar affinity. Preliminary crystallographic data indicates that the aptamer stabilizes a distinct inactive conformation of the kinase domain similar to that recognized by the Takeda compounds. In Chapter 5, we have developed a displacement assay using a related aptamer in the format of a FCPIA that is currently in use to screen for small molecule inhibitors that bind to the inactive kinase conformation. Based on the selectivity profiles of the aptamer and that of the Takeda compounds, we expect to potentially discover GRK2 inhibitors that have similar selectivity profiles. Pending the success of this screen, the use of enigineered RNA aptamers could become a common tool for developing selective kinase inhibitors.

References

1. Schoneberg, T., Schulz, A., Biebermann, H., Hermsdorf, T., Rompler, H., and Sangkuhl, K. (2004) Mutant G-protein-coupled receptors as a cause of human diseases, *Pharmacol Ther 104*, 173-206.
2. Overington, J. P., Al-Lazikani, B., and Hopkins, A. L. (2006) How many drug targets are there?, *Nat Rev Drug Discov 5*, 993-996.
3. Wise, A., Gearing, K., and Rees, S. (2002) Target validation of G-protein coupled receptors, *Drug Discovery Today 7*, 235-246.
4. Oldham, W. M., and Hamm, H. E. (2008) Heterotrimeric G protein activation by G-protein-coupled receptors, *Nat Rev Mol Cell Biol 9*, 60-71.
5. Pierce, K. L., Premont, R. T., and Lefkowitz, R. J. (2002) Seven-transmembrane receptors, *Nat Rev Mol Cell Biol 3*, 639-650.
6. Strader, C. D., Fong, T. M., Tota, M. R., Underwood, D., and Dixon, R. A. F. (2003) Structure and Function of G Protein-Coupled Receptors, *Annual Review of Biochemistry 63*, 101-132.
7. Foord, S. M., Bonner, T. I., Neubig, R. R., Rosser, E. M., Pin, J.-P., Davenport, A. P., Spedding, M., and Harmar, A. J. (2005) International Union of Pharmacology. XLVI. G Protein-Coupled Receptor List, *Pharmacological Reviews 57*, 279-288.
8. Rovati, G. E., Capra, V. r., and Neubig, R. R. (2007) The Highly Conserved DRY Motif of Class A G Protein-Coupled Receptors: Beyond the Ground State, *Molecular Pharmacology 71*, 959-964.
9. Gilman, A. G. (1987) G Proteins: Transducers of Receptor-Generated Signals, *Annual Review of Biochemistry 56*, 615-649.
10. Kristiansen, K. (2004) Molecular mechanisms of ligand binding, signaling, and regulation within the superfamily of G-protein-coupled receptors: molecular modeling and mutagenesis approaches to receptor structure and function, *Pharmacology & Therapeutics 103*, 21-80.
11. Oldham, W. M., and Hamm, H. E. (2006) Structural basis of function in heterotrimeric G proteins, *Q Rev Biophys 39*, 117-166.
12. Ross, E. M., and Wilkie, T. M. (2003) GTPASE-ACTIVATING PROTEINS FOR HETEROTRIMERIC G PROTEINS: Regulators of G Protein Signaling (RGS) and RGS-Like Proteins, *Annual Review of Biochemistry 69*, 795-827.
13. Pitcher, J. A., Freedman, N. J., and Lefkowitz, R. J. (1998) G PROTEIN COUPLED RECEPTOR KINASES, *Annual Review of Biochemistry 67*, 653-692.
14. Gainetdinov, R. R., Premont, R. T., Bohn, L. M., Lefkowitz, R. J., and Caron, M. G. (2004) Desensitization of G protein-coupled receptors and neuronal functions, *Annu Rev Neurosci 27*, 107-144.

15. Krupnick, J. G., and Benovic, J. L. (1998) The role of receptor kinases and arrestins in G protein-coupled receptor regulation, *Annu Rev Pharmacol Toxicol 38*, 289-319.
16. Sprang, S. R., Chen, Z., and Du, X. (2007) Structural basis of effector regulation and signal termination in heterotrimeric Gα proteins, *Adv Protein Chem 74*, 1-65.
17. Sprang, S. R. (1997) G protein mechanisms: insights from structural analysis, *Annu Rev Biochem 66*, 639-678.
18. Kreutz, B., Yau, D. M., Nance, M. R., Tanabe, S., Tesmer, J. J., and Kozasa, T. (2006) A new approach to producing functional G alpha subunits yields the activated and deactivated structures of G alpha(12/13) proteins, *Biochemistry 45*, 167-174.
19. Hubbard, K. B., and Hepler, J. R. (2006) Cell signalling diversity of the Gqalpha family of heterotrimeric G proteins, *Cell Signal 18*, 135-150.
20. Offermanns, S., Toombs, C. F., Hu, Y. H., and Simon, M. I. (1997) Defective platelet activation in $G\alpha_q$-deficient mice, *Nature 389*, 183-186.
21. Aittaleb, M., Boguth, C. A., and Tesmer, J. J. (2010) Structure and function of heterotrimeric G protein-regulated Rho guanine nucleotide exchange factors, *Mol Pharmacol 77*, 111-125.
22. Simon, M. I., Strathmann, M. P., and Gautam, N. (1991) Diversity of G proteins in signal transduction, *Science 252*, 802-808.
23. Hepler, J. R., and Gilman, A. G. (1992) G proteins, *Trends Biochem Sci 17*, 383-387.
24. Lutz, S., Shankaranarayanan, A., Coco, C., Ridilla, M., Nance, M. R., Vettel, C., Baltus, D., Evelyn, C. R., Neubig, R. R., Wieland, T., and Tesmer, J. J. (2007) Structure of $G\alpha_q$-p63RhoGEF-RhoA complex reveals a pathway for the activation of RhoA by GPCRs, *Science 318*, 1923-1927.
25. Sallese, M., Mariggio, S., D'Urbano, E., Iacovelli, L., and De Blasi, A. (2000) Selective regulation of G_q signaling by G protein-coupled receptor kinase 2: direct interaction of kinase N terminus with activated $G\alpha_q$, *Mol Pharmacol 57*, 826-831.
26. Tesmer, V. M., Kawano, T., Shankaranarayanan, A., Kozasa, T., and Tesmer, J. J. (2005) Snapshot of activated G proteins at the membrane: the $G\alpha_q$-GRK2-Gβγ complex, *Science 310*, 1686-1690.
27. Day, P. W., Carman, C. V., Sterne-Marr, R., Benovic, J. L., and Wedegaertner, P. B. (2003) Differential interaction of GRK2 with members of the $G\alpha_q$ family, *Biochemistry 42*, 9176-9184.
28. Usui, H., Nishiyama, M., Moroi, K., Shibasaki, T., Zhou, J., Ishida, J., Fukamizu, A., Haga, T., Sekiya, S., and Kimura, S. (2000) RGS domain in the amino-terminus of G protein-coupled receptor kinase 2 inhibits G_q-mediated signaling, *Int J Mol Med 5*, 335-340.
29. Carman, C. V., Parent, J. L., Day, P. W., Pronin, A. N., Sternweis, P. M., Wedegaertner, P. B., Gilman, A. G., Benovic, J. L., and Kozasa, T. (1999) Selective regulation of $G\alpha_{q/11}$ by an RGS domain in the G protein- coupled receptor kinase, GRK2, *J Biol Chem 274*, 34483-34492.

30. Tall, G. G., Krumins, A. M., and Gilman, A. G. (2003) Mammalian Ric-8A (synembryn) is a heterotrimeric Galpha protein guanine nucleotide exchange factor, *J Biol Chem 278*, 8356-8362.
31. Nishimura, A., Okamoto, M., Sugawara, Y., Mizuno, N., Yamauchi, J., and Itoh, H. (2006) Ric-8A potentiates Gq-mediated signal transduction by acting downstream of G protein-coupled receptor in intact cells, *Genes Cells 11*, 487-498.
32. Popova, J. S., Garrison, J. C., Rhee, S. G., and Rasenick, M. M. (1997) Tubulin, Gq, and phosphatidylinositol 4,5-bisphosphate interact to regulate phospholipase Cbeta1 signaling, *J Biol Chem 272*, 6760-6765.
33. Popova, J. S., and Rasenick, M. M. (2000) Muscarinic receptor activation promotes the membrane association of tubulin for the regulation of Gq-mediated phospholipase Cbeta(1) signaling, *J Neurosci 20*, 2774-2782.
34. Oh, P., and Schnitzer, J. E. (2001) Segregation of heterotrimeric G proteins in cell surface microdomains. G(q) binds caveolin to concentrate in caveolae, whereas G(i) and G(s) target lipid rafts by default, *Mol Biol Cell 12*, 685-698.
35. Bence, K., Ma, W., Kozasa, T., and Huang, X. Y. (1997) Direct stimulation of Bruton's tyrosine kinase by G(q)-protein alpha-subunit, *Nature 389*, 296-299.
36. Ballou, L. M., Chattopadhyay, M., Li, Y., Scarlata, S., and Lin, R. Z. (2006) Galphaq binds to p110alpha/p85alpha phosphoinositide 3-kinase and displaces Ras, *Biochem J 394*, 557-562.
37. Jalili, T., Takeishi, Y., and Walsh, R. A. (1999) Signal transduction during cardiac hypertrophy: the role of G alpha q, PLC beta I, and PKC, *Cardiovasc Res 44*, 5-9.
38. Offermanns, S., Zhao, L. P., Gohla, A., Sarosi, I., Simon, M. I., and Wilkie, T. M. (1998) Embryonic cardiomyocyte hypoplasia and craniofacial defects in $G\alpha_q$/$G\alpha_{11}$-mutant mice, *Embo J 17*, 4304-4312.
39. Moers, A., Wettschureck, N., Gruner, S., Nieswandt, B., and Offermanns, S. (2004) Unresponsiveness of platelets lacking both Galpha(q) and Galpha(13). Implications for collagen-induced platelet activation, *J Biol Chem 279*, 45354-45359.
40. Adams, J. W., and Brown, J. H. (2001) G-proteins in growth and apoptosis: lessons from the heart, *Oncogene 20*, 1626-1634.
41. Offermanns, S., Hashimoto, K., Watanabe, M., Sun, W., Kurihara, H., Thompson, R. F., Inoue, Y., Kano, M., and Simon, M. I. (1997) Impaired motor coordination and persistent multiple climbing fiber innervation of cerebellar Purkinje cells in mice lacking $G\alpha_q$, *Proc Natl Acad Sci U S A 94*, 14089-14094.
42. Borchers, M. T., Biechele, T., Justice, J. P., Ansay, T., Cormier, S., Mancino, V., Wilkie, T. M., Simon, M. I., Lee, N. A., and Lee, J. J. (2003) Methacholine-induced airway hyperresponsiveness is dependent on Galphaq signaling, *Am J Physiol Lung Cell Mol Physiol 285*, L114-120.

43. Baltensperger, K., and Porzig, H. (1997) The P2U purinoceptor obligatorily engages the heterotrimeric G protein G16 to mobilize intracellular Ca2+ in human erythroleukemia cells, *J Biol Chem 272*, 10151-10159.
44. Lambright, D. G., Noel, J. P., Hamm, H. E., and Sigler, P. B. (1994) Structural determinants for activation of the α-subunit of a heterotrimeric G protein, *Nature 369*, 621-628.
45. Mixon, M. B., Lee, E., Coleman, D. E., Berghuis, A. M., Gilman, A. G., and Sprang, S. R. (1995) Tertiary and quaternary structural changes in $G_{i\alpha 1}$ induced by GTP hydrolysis., *Science 270*, 954-960.
46. Berghuis, A. M., Lee, E., Raw, A. S., Gilman, A. G., and Sprang, S. R. (1996) Structure of the GDP-Pi complex of Gly203-->Ala $G_{i\alpha 1}$: a mimic of the ternary product complex of G_{α}-catalyzed GTP hydrolysis., *Structure 4*, 1277-1290.
47. Raw, A. S., Coleman, D. E., Gilman, A. G., and Sprang, S. R. (1997) *Biochemistry*, In the press.
48. Noel, J. P., Hamm, H. E., and Sigler, P. B. (1993) The 2.2 A crystal structure of transducin-alpha complexed with GTPγS., *Nature 366*, 654-663.
49. Coleman, D. E., Berghuis, A. M., Lee, E., Linder, M. E., Gilman, A. G., and Sprang, S. R. (1994) Structures of active conformations of $G_{i\alpha 1}$ and the mechanism of GTP hydrolysis., *Science 265*, 1405-1412.
50. Sondek, J., Lambright, D. G., Noel, J. P., Hamm, H. E., and Sigler, P. B. (1994) GTPase mechanism of G proteins from the 1.7 Å crystal structure of transducin α-GDP-AlF_4^-. *Nature 372*, 276-279.
51. Brandt, D. R., and Ross, E. M. (1985) GTPase activity of the stimulatory GTP-binding regulatory protein of adenylate cyclase, G_s. Accumulation and turnover of enzyme-nucleotide intermediates, *J Biol Chem 260*, 266-272.
52. Arshavsky, V., and Bownds, M. D. (1992) Regulation of deactivation of photoreceptor G protein by its target enzyme and cGMP, *Nature 357*, 416-417.
53. Berman, D. M., Wilkie, T. M., and Gilman, A. G. (1996) GAIP and RGS4 are GTPase-activating proteins (GAPs) for the G_i subfamily of G protein α subunits, *Cell 86*, 445-452.
54. Hunt, T. W., Fields, T. A., Casey, P. J., and Peralta, E. G. (1996) RGS10 is a selective activator of $G_{i\alpha}$ GTPase activity, *Nature 383*, 175-177.
55. Watson, N., Linder, M. E., Druey, K. M., Kehrl, J. H., and Blumer, K. J. (1996) RGS family members: GTPase-activating proteins for heterotrimeric G-protein α-subunits, *Nature 383*, 172-175.
56. Hollinger, S., and Hepler, J. R. (2002) Cellular regulation of RGS proteins: modulators and integrators of G protein signaling, *Pharmacol Rev 54*, 527-559.
57. Hepler, J. R. (1999) Emerging roles for RGS proteins in cell signalling, *Trends Pharmacol Sci 20*, 376-382.

58. Tesmer, J. J. (2009) Chapter 4 Structure and Function of Regulator of G Protein Signaling Homology Domains, *Prog Mol Biol Transl Sci 86C*, 75-113.
59. Tesmer, J. J., Berman, D. M., Gilman, A. G., and Sprang, S. R. (1997) Structure of RGS4 bound to AlF4--activated G(i alpha1): stabilization of the transition state for GTP hydrolysis, *Cell 89*, 251-261.
60. Posner, B. A., Mukhopadhyay, S., Tesmer, J. J., Gilman, A. G., and Ross, E. M. (1999) Modulation of the affinity and selectivity of RGS protein interaction with G alpha subunits by a conserved asparagine/serine residue, *Biochemistry 38*, 7773-7779.
61. Natochin, M., McEntaffer, R. L., and Artemyev, N. O. (1998) Mutational analysis of the Asn residue essential for RGS protein binding to G-proteins, *J Biol Chem 273*, 6731-6735.
62. Soundararajan, M., Willard, F. S., Kimple, A. J., Turnbull, A. P., Ball, L. J., Schoch, G. A., Gileadi, C., Fedorov, O. Y., Dowler, E. F., Higman, V. A., Hutsell, S. Q., Sundstrom, M., Doyle, D. A., and Siderovski, D. P. (2008) Structural diversity in the RGS domain and its interaction with heterotrimeric G protein α-subunits, *Proc Natl Acad Sci U S A 105*, 6457-6462.
63. Heximer, S. P., Srinivasa, S. P., Bernstein, L. S., Bernard, J. L., Linder, M. E., Hepler, J. R., and Blumer, K. J. (1999) G protein selectivity is a determinant of RGS2 function, *J Biol Chem 274*, 34253-34259.
64. Heximer, S. P., Watson, N., Linder, M. E., Blumer, K. J., and Hepler, J. R. (1997) RGS2/G0S8 is a selective inhibitor of $G_q\alpha$ function, *Proc Natl Acad Sci U S A 94*, 14389-14393.
65. Palczewski, K., and Benovic, J. L. (1991) G-protein-coupled receptor kinases, *Trends Biochem Sci 16*, 387-391.
66. Carman, C. V., Barak, L. S., Chen, C., Liu-Chen, L. Y., Onorato, J. J., Kennedy, S. P., Caron, M. G., and Benovic, J. L. (2000) Mutational analysis of G$\beta\gamma$ and phospholipid interaction with G protein-coupled receptor kinase 2, *J Biol Chem 275*, 10443-10452.
67. Oppermann, M., Freedman, N. J., Alexander, R. W., and Lefkowitz, R. J. (1996) Phosphorylation of the type 1A angiotensin II receptor by G protein- coupled receptor kinases and protein kinase C, *J Biol Chem 271*, 13266-13272.
68. Freedman, N. J., Ament, A. S., Oppermann, M., Stoffel, R. H., Exum, S. T., and Lefkowitz, R. J. (1997) Phosphorylation and desensitization of human endothelin A and B receptors. Evidence for G protein-coupled receptor kinase specificity, *J Biol Chem 272*, 17734-17743.
69. Dicker, F., Quitterer, U., Winstel, R., Honold, K., and Lohse, M. J. (1999) Phosphorylation-independent inhibition of parathyroid hormone receptor signaling by G protein-coupled receptor kinases, *Proc Natl Acad Sci U S A 96*, 5476-5481.
70. Willets, J. M., Nahorski, S. R., and Challiss, R. A. (2005) Roles of Phosphorylation-dependent and -independent Mechanisms in the Regulation of M1 Muscarinic Acetylcholine Receptors by G Protein-

coupled Receptor Kinase 2 in Hippocampal Neurons, *J Biol Chem 280*, 18950-18958.
71. Dhami, G. K., Dale, L. B., Anborgh, P. H., O'Connor-Halligan, K. E., Sterne-Marr, R., and Ferguson, S. S. (2004) G Protein-coupled receptor kinase 2 regulator of G protein signaling homology domain binds to both metabotropic glutamate receptor 1a and $G\alpha_q$ to attenuate signaling, *J Biol Chem 279*, 16614-16620.
72. Dhami, G. K., Anborgh, P. H., Dale, L. B., Sterne-Marr, R., and Ferguson, S. S. (2002) Phosphorylation-independent regulation of metabotropic glutamate receptor signaling by G protein-coupled receptor kinase 2, *J Biol Chem 277*, 25266-25272.
73. Shankaranarayanan, A., Thal, D. M., Tesmer, V. M., Roman, D. L., Neubig, R. R., Kozasa, T., and Tesmer, J. J. (2008) Assembly of high order $G\alpha_q$-effector complexes with RGS proteins, *J Biol Chem 283*, 34923-34934.
74. Day, P. W., Tesmer, J. J., Sterne-Marr, R., Freeman, L. C., Benovic, J. L., and Wedegaertner, P. B. (2004) Characterization of the GRK2 binding site of $G\alpha_q$, *J Biol Chem 279*, 53643-53652.
75. Sterne-Marr, R., Tesmer, J. J., Day, P. W., Stracquatanio, R. P., Cilente, J. A., O'Connor, K. E., Pronin, A. N., Benovic, J. L., and Wedegaertner, P. B. (2003) G protein-coupled receptor Kinase 2/G alpha q/11 interaction. A novel surface on a regulator of G protein signaling homology domain for binding G alpha subunits, *J Biol Chem 278*, 6050-6058.
76. Tesmer, J. J., Sunahara, R. K., Gilman, A. G., and Sprang, S. R. (1997) Crystal structure of the catalytic domains of adenylyl cyclase in a complex with $G_{s\alpha}$·GTPγS, *Science 278*, 1907-1916.
77. Slep, K. C., Kercher, M. A., He, W., Cowan, C. W., Wensel, T. G., and Sigler, P. B. (2001) Structural determinants for regulation of phosphodiesterase by a G protein at 2.0 Å, *Nature 409*, 1071-1077.
78. Chen, Z., Singer, W. D., Sternweis, P. C., and Sprang, S. R. (2005) Structure of the p115RhoGEF rgRGS domain-$G\alpha_{13/i1}$ chimera complex suggests convergent evolution of a GTPase activator, *Nat Struct Mol Biol 12*, 191-197.
79. Tolkovsky, A. M., and Levitzki, A. (1978) Mode of coupling between the beta-adrenergic receptor and adenylate cyclase in turkey erythrocytes, *Biochemistry 17*, 3795.
80. Yamada, M., Inanobe, A., and Kurachi, Y. (1998) G protein regulation of potassium ion channels, *Pharmacol Rev 50*, 723-760.
81. Rebois, R. V., and Hebert, T. E. (2003) Protein complexes involved in heptahelical receptor-mediated signal transduction, *Receptors Channels 9*, 169-194.
82. Biddlecome, G. H., Berstein, G., and Ross, E. M. (1996) Regulation of phospholipase C-beta1 by Gq and m1 muscarinic cholinergic receptor. Steady-state balance of receptor-mediated activation and GTPase-activating protein-promoted deactivation, *J Biol Chem 271*, 7999-8007.

83. Zhong, H., Wade, S. M., Woolf, P. J., Linderman, J. J., Traynor, J. R., and Neubig, R. R. (2003) A spatial focusing model for G protein signals. Regulator of G protein signaling (RGS) protien-mediated kinetic scaffolding, *J Biol Chem 278*, 7278-7284.
84. He, W., Cowan, C. W., and Wensel, T. G. (1998) RGS9, a GTPase accelerator for phototransduction, *Neuron 20*, 95-102.
85. McEntaffer, R. L., Natochin, M., and Artemyev, N. O. (1999) Modulation of transducin GTPase activity by chimeric RGS16 and RGS9 regulators of G protein signaling and the effector molecule, *Biochemistry 38*, 4931-4937.
86. Skiba, N. P., Yang, C. S., Huang, T., Bae, H., and Hamm, H. E. (1999) The α-helical domain of $G\alpha_t$ determines specific interaction with regulator of G protein signaling 9, *J Biol Chem 274*, 8770-8778.
87. Nekrasova, E., Berman, D., Rustandi, R., Hamm, H., Gilman, A., and Arshavsky, V. (1997) Activation of transducin guanosine triphosphatase by two proteins of the RGS family., *Biochemistry 36*, 7638-7643.
88. Natochin, M., Granovsky, A. E., and Artemyev, N. O. (1997) Regulation of transducin GTPase activity by human retinal RGS, *J Biol Chem 272*, 17444-17449.
89. Wieland, T., Chen, C. K., and Simon, M. I. (1997) The retinal specific protein RGS-r competes with the γ subunit of cGMP phosphodiesterase for the α subunit of transducin and facilitates signal termination, *J Biol Chem 272*, 8853-8856.
90. Usui, I., Imamura, T., Babendure, J. L., Satoh, H., Lu, J. C., Hupfeld, C. J., and Olefsky, J. M. (2005) G protein-coupled receptor kinase 2 mediates endothelin-1-induced insulin resistance via the inhibition of both Galphaq/11 and insulin receptor substrate-1 pathways in 3T3-L1 adipocytes, *Mol Endocrinol 19*, 2760-2768.
91. Peregrin, S., Jurado-Pueyo, M., Campos, P. M., Sanz-Moreno, V., Ruiz-Gomez, A., Crespo, P., Mayor, F., Jr., and Murga, C. (2006) Phosphorylation of p38 by GRK2 at the docking groove unveils a novel mechanism for inactivating p38MAPK, *Curr Biol 16*, 2042-2047.
92. Cant, S. H., and Pitcher, J. A. (2005) G protein-coupled receptor kinase 2-mediated phosphorylation of ezrin is required for G protein-coupled receptor-dependent reorganization of the actin cytoskeleton, *Mol Biol Cell 16*, 3088-3099.
93. Ross, E. M., and Wilkie, T. M. (2000) GTPase-activating proteins for heterotrimeric G proteins: regulators of G protein signaling (RGS) and RGS-like proteins, *Annu Rev Biochem 69*, 795-827.
94. Bansal, G., Druey, K. M., and Xie, Z. (2007) R4 RGS proteins: regulation of G-protein signaling and beyond, *Pharmacol Ther 116*, 473-495.
95. Hepler, J. R., Berman, D. M., Gilman, A. G., and Kozasa, T. (1997) RGS4 and GAIP are GTPase-activating proteins for $G_{q\alpha}$ and block activation of phospholipase Cβ by γ-thio-GTP-$G_{q\alpha}$, *Proc Natl Acad Sci U S A 94*, 428-432.

96. Anger, T., Zhang, W., and Mende, U. (2004) Differential contribution of GTPase activation and effector antagonism to the inhibitory effect of RGS proteins on Gq-mediated signaling in vivo, *J Biol Chem 279*, 3906-3915.
97. Kristelly, R., Earnest, B. T., Krishnamoorthy, L., and Tesmer, J. J. (2003) Preliminary structure analysis of the DH/PH domains of leukemia-associated RhoGEF, *Acta Crystallogr D Biol Crystallogr 59*, 1859-1862.
98. Heximer, S. P. (2004) RGS2-mediated regulation of Gqalpha, *Methods Enzymol 390*, 65-82.
99. Tesmer, J. J., Berman, D. M., Gilman, A. G., and Sprang, S. R. (1997) Structure of RGS4 bound to AlF_4^--activated $G_{i\alpha 1}$: stabilization of the transition state for GTP hydrolysis, *Cell 89*, 251-261.
100. Lodowski, D. T., Barnhill, J. F., Pitcher, J. A., Capel, W. D., Lefkowitz, R. J., and Tesmer, J. J. (2003) Purification, crystallization and preliminary X-ray diffraction studies of a complex between G protein-coupled receptor kinase 2 and Gbeta1gamma2, *Acta Crystallogr D Biol Crystallogr 59*, 936-939.
101. Ehlert, F. J. (1988) Estimation of the affinities of allosteric ligands using radioligand binding and pharmacological null methods, *Mol Pharmacol 33*, 187-194.
102. Roman, D. L., Talbot, J. N., Roof, R. A., Sunahara, R. K., Traynor, J. R., and Neubig, R. R. (2007) Identification of small-molecule inhibitors of RGS4 using a high-throughput flow cytometry protein interaction assay, *Mol Pharmacol 71*, 169-175.
103. Gu, S., He, J., Ho, W. T., Ramineni, S., Thal, D. M., Natesh, R., Tesmer, J. J., Hepler, J. R., and Heximer, S. P. (2007) Unique hydrophobic extension of the RGS2 amphipathic helix domain imparts increased plasma membrane binding and function relative to other RGS R4/B subfamily members, *J Biol Chem 282*, 33064-33075.
104. Kreutz, B., Yau, D. M., Nance, M. R., Tanabe, S., Tesmer, J. J., and Kozasa, T. (2006) A new approach to producing functional Gα subunits yields the activated and deactivated structures of $G\alpha_{12/13}$ proteins, *Biochemistry 45*, 167-174.
105. Posner, B. A., Mukhopadhyay, S., Tesmer, J. J., Gilman, A. G., and Ross, E. M. (1999) Modulation of the affinity and selectivity of RGS protein interaction with $G\alpha$ subunits by a conserved asparagine/serine residue, *Biochemistry 38*, 7773-7779.
106. Zeng, W., Xu, X., Popov, S., Mukhopadhyay, S., Chidiac, P., Swistok, J., Danho, W., Yagaloff, K. A., Fisher, S. L., Ross, E. M., Muallem, S., and Wilkie, T. M. (1998) The N-terminal domain of RGS4 confers receptor-selective inhibition of G protein signaling, *J Biol Chem 273*, 34687-34690.
107. Chen, C., Seow, K. T., Guo, K., Yaw, L. P., and Lin, S. C. (1999) The membrane association domain of RGS16 contains unique amphipathic features that are conserved in RGS4 and RGS5, *J Biol Chem 274*, 19799-19806.

108. Bernstein, L. S., Grillo, A. A., Loranger, S. S., and Linder, M. E. (2000) RGS4 binds to membranes through an amphipathic α-helix, *J Biol Chem 275*, 18520-18526.
109. Bernstein, L. S., Ramineni, S., Hague, C., Cladman, W., Chidiac, P., Levey, A. I., and Hepler, J. R. (2004) RGS2 binds directly and selectively to the M1 muscarinic acetylcholine receptor third intracellular loop to modulate $G_{q/11}\alpha$ signaling, *J Biol Chem 279*, 21248-21256.
110. Salim, S., Sinnarajah, S., Kehrl, J. H., and Dessauer, C. W. (2003) Identification of RGS2 and type V adenylyl cyclase interaction sites, *J Biol Chem 278*, 15842-15849.
111. Schoeber, J. P., Topala, C. N., Wang, X., Diepens, R. J., Lambers, T. T., Hoenderop, J. G., and Bindels, R. J. (2006) RGS2 inhibits the epithelial Ca2+ channel TRPV6, *J Biol Chem 281*, 29669-29674.
112. Lutz, S., Shankaranarayanan, A., Coco, C., Ridilla, M., Nance, M. R., Vettel, C., Baltus, D., Evelyn, C. R., Neubig, R. R., Wieland, T., and Tesmer, J. J. (2007) Structure of Galphaq-p63RhoGEF-RhoA complex reveals a pathway for the activation of RhoA by GPCRs, *Science 318*, 1923-1927.
113. Christopoulos, A., and Kenakin, T. (2002) G protein-coupled receptor allosterism and complexing, *Pharmacol Rev 54*, 323-374.
114. Chidiac, P., Markin, V. S., and Ross, E. M. (1999) Kinetic control of guanine nucleotide binding to soluble $G\alpha_q$, *Biochem Pharmacol 58*, 39-48.
115. Conklin, B. R., Chabre, O., Wong, Y. H., Federman, A. D., and Bourne, H. R. (1992) Recombinant Gq alpha. Mutational activation and coupling to receptors and phospholipase C., *J Biol Chem 267*, 31-34.
116. Arshavsky, V. Y., and Pugh, E. N., Jr. (1998) Lifetime regulation of G protein-effector complex: emerging importance of RGS proteins, *Neuron 20*, 11-14.
117. Arshavsky, V. Y., Lamb, T. D., and Pugh, E. N., Jr. (2002) G proteins and phototransduction, *Annu Rev Physiol 64*, 153-187.
118. Cook, B., Bar-Yaacov, M., Cohen Ben-Ami, H., Goldstein, R. E., Paroush, Z., Selinger, Z., and Minke, B. (2000) Phospholipase C and termination of G-protein-mediated signalling in vivo, *Nat Cell Biol 2*, 296-301.
119. Mukhopadhyay, S., and Ross, E. M. (1999) Rapid GTP binding and hydrolysis by G(q) promoted by receptor and GTPase-activating proteins, *Proc Natl Acad Sci U S A 96*, 9539-9544.
120. Ranganathan, R., Harris, G. L., Stevens, C. F., and Zuker, C. S. (1991) A Drosophila mutant defective in extracellular calcium-dependent photoreceptor deactivation and rapid desensitization, *Nature 354*, 230-232.
121. Sterne-Marr, R., Tesmer, J. J., Day, P. W., Stracquatanio, R. P., Cilente, J. A., O'Connor, K. E., Pronin, A. N., Benovic, J. L., and Wedegaertner, P. B. (2003) G protein-coupled receptor Kinase 2/$G\alpha_{q/11}$ interaction. A novel surface on a regulator of G protein signaling homology domain for binding Gα subunits, *J Biol Chem 278*, 6050-6058.

122. Koch, W. J., Hawes, B. E., Inglese, J., Luttrell, L. M., and Lefkowitz, R. J. (1994) Cellular expression of the carboxyl terminus of a G protein-coupled receptor kinase attenuates G beta gamma-mediated signaling, *J Biol Chem 269*, 6193-6197.
123. Koch, W. J., Rockman, H. A., Samama, P., Hamilton, R. A., Bond, R. A., Milano, C. A., and Lefkowitz, R. J. (1995) Cardiac function in mice overexpressing the beta-adrenergic receptor kinase or a beta ARK inhibitor, *Science 268*, 1350-1353.
124. Adams, J. W., Sakata, Y., Davis, M. G., Sah, V. P., Wang, Y., Liggett, S. B., Chien, K. R., Brown, J. H., and Dorn, G. W., 2nd. (1998) Enhanced $G\alpha_q$ signaling: a common pathway mediates cardiac hypertrophy and apoptotic heart failure, *Proc Natl Acad Sci U S A 95*, 10140-10145.
125. D'Angelo, D. D., Sakata, Y., Lorenz, J. N., Boivin, G. P., Walsh, R. A., Liggett, S. B., and Dorn, G. W., 2nd. (1997) Transgenic $G\alpha_q$ overexpression induces cardiac contractile failure in mice, *Proc Natl Acad Sci U S A 94*, 8121-8126.
126. Dorn, G. W., 2nd, and Hahn, H. S. (2004) Genetic factors in cardiac hypertrophy, *Ann N Y Acad Sci 1015*, 225-237.
127. LaMorte, V. J., Thorburn, J., Absher, D., Spiegel, A., Brown, J. H., Chien, K. R., Feramisco, J. R., and Knowlton, K. U. (1994) G_q- and ras-dependent pathways mediate hypertrophy of neonatal rat ventricular myocytes following α_1-adrenergic stimulation, *J Biol Chem 269*, 13490-13496.
128. Offermanns, S., and Simon, M. I. (1998) Genetic analysis of mammalian G-protein signalling, *Oncogene 17*, 1375-1381.
129. Lutz, S., Freichel-Blomquist, A., Yang, Y., Rumenapp, U., Jakobs, K. H., Schmidt, M., and Wieland, T. (2005) The guanine nucleotide exchange factor p63RhoGEF, a specific link between $G_{q/11}$-coupled receptor signaling and RhoA, *J Biol Chem 280*, 11134-11139.
130. Shankaranarayanan, A., Thal, D. M., Tesmer, V. M., Roman, D. L., Neubig, R. R., Kozasa, T., and Tesmer, J. J. (2008) Assembly of high order G alpha q-effector complexes with RGS proteins, *J Biol Chem 283*, 34923-34934.
131. Penela, P., Murga, C., Ribas, C., Lafarga, V., and Mayor, F., Jr. (2010) The complex G protein-coupled receptor kinase 2 (GRK2) interactome unveils new physiopathological targets, *Br J Pharmacol 160*, 821-832.
132. Wells, J. A., and McClendon, C. L. (2007) Reaching for high-hanging fruit in drug discovery at protein-protein interfaces, *Nature 450*, 1001-1009.
133. Arkin, M. R., and Wells, J. A. (2004) Small-molecule inhibitors of protein-protein interactions: progressing towards the dream, *Nat Rev Drug Discov 3*, 301-317.
134. Blazer, L. L., and Neubig, R. R. (2009) Small molecule protein-protein interaction inhibitors as CNS therapeutic agents: current progress and future hurdles, *Neuropsychopharmacology 34*, 126-141.
135. Cochran, A. G. (2000) Antagonists of protein-protein interactions, *Chem Biol 7*, R85-94.

136. Spencer, R. W. (1998) High-throughput screening of historic collections: observations on file size, biological targets, and file diversity, *Biotechnol Bioeng 61*, 61-67.
137. Bogan, A. A., and Thorn, K. S. (1998) Anatomy of hot spots in protein interfaces, *J Mol Biol 280*, 1-9.
138. Wells, J. A. (1991) Systematic mutational analyses of protein-protein interfaces, *Methods Enzymol 202*, 390-411.
139. Tesmer, J. J. (2006) Pharmacology. Hitting the hot spots of cell signaling cascades, *Science 312*, 377-378.
140. Bonacci, T. M., Mathews, J. L., Yuan, C., Lehmann, D. M., Malik, S., Wu, D., Font, J. L., Bidlack, J. M., and Smrcka, A. V. (2006) Differential targeting of Gbetagamma-subunit signaling with small molecules, *Science 312*, 443-446.
141. Davis, T. L., Bonacci, T. M., Sprang, S. R., and Smrcka, A. V. (2005) Structural and molecular characterization of a preferred protein interaction surface on G protein βγ subunits, *Biochemistry 44*, 10593-10604.
142. Scott, J. K., Huang, S.-F., Gangadhar, B. P., Samoriski, G. M., Clapp, P., Gross, R. A., Taussig, R., and Smrcka, A. V. (2001) Evidence that a protein‚Äìprotein interaction 'hot spot' on heterotrimeric G protein [beta][gamma] subunits is used for recognition of a subclass of effectors, *EMBO J 20*, 767-776.
143. Takasaki, J., Saito, T., Taniguchi, M., Kawasaki, T., Moritani, Y., Hayashi, K., and Kobori, M. (2004) A novel Galphaq/11-selective inhibitor, *J Biol Chem 279*, 47438-47445.
144. Nishimura A Fau - Kitano, K., Kitano K Fau - Takasaki, J., Takasaki J Fau - Taniguchi, M., Taniguchi M Fau - Mizuno, N., Mizuno N Fau - Tago, K., Tago K Fau - Hakoshima, T., Hakoshima T Fau - Itoh, H., and Itoh, H. Structural basis for the specific inhibition of heterotrimeric Gq protein by a small molecule.
145. Blazer, L. L., Roman, D. L., Chung, A., Larsen, M. J., Greedy, B. M., Husbands, S. M., and Neubig, R. R. (2010) Reversible, allosteric small-molecule inhibitors of regulator of g protein signaling proteins, *Mol Pharmacol 78*, 524-533.
146. Kimple, A. J., Willard, F. S., Giguere, P. M., Johnston, C. A., Mocanu, V., and Siderovski, D. P. (2007) The RGS protein inhibitor CCG-4986 is a covalent modifier of the RGS4 Galpha-interaction face, *Biochim Biophys Acta 1774*, 1213-1220.
147. Roman, D. L., Blazer, L. L., Monroy, C. A., and Neubig, R. R. (2010) Allosteric Inhibition of the Regulator of G Protein Signaling-G{alpha} Protein-Protein Interaction by CCG-4986, *Mol Pharmacol 78*, 360-365.
148. Roof, R. A., Jin, Y., Roman, D. L., Sunahara, R. K., Ishii, M., Mosberg, H. I., and Neubig, R. R. (2006) Mechanism of action and structural requirements of constrained peptide inhibitors of RGS proteins, *Chem Biol Drug Des 67*, 266-274.
149. Roof, R. A., Roman, D. L., Clements, S. T., Sobczyk-Kojiro, K., Blazer, L. L., Ota, S., Mosberg, H. I., and Neubig, R. R. (2009) A covalent peptide

inhibitor of RGS4 identified in a focused one-bead, one compound library screen, *BMC Pharmacol 9*, 9.
150. Roof, R. A., Sobczyk-Kojiro, K., Turbiak, A. J., Roman, D. L., Pogozheva, I. D., Blazer, L. L., Neubig, R. R., and Mosberg, H. I. (2008) Novel peptide ligands of RGS4 from a focused one-bead, one-compound library, *Chem Biol Drug Des 72*, 111-119.
151. Roman, D. L., Ota, S., and Neubig, R. R. (2009) Polyplexed flow cytometry protein interaction assay: a novel high-throughput screening paradigm for RGS protein inhibitors, *J Biomol Screen 14*, 610-619.
152. Tall, G. G., and Gilman, A. G. (2004) Purification and functional analysis of Ric-8A: a guanine nucleotide exchange factor for G-protein alpha subunits, *Methods Enzymol 390*, 377-388.
153. Pitcher, J. A., Tesmer, J. J., Freeman, J. L., Capel, W. D., Stone, W. C., and Lefkowitz, R. J. (1999) Feedback inhibition of G protein-coupled receptor kinase 2 (GRK2) activity by extracellular signal-regulated kinases, *J Biol Chem 274*, 34531-34534.
154. Blazer, L. L., Roman, D. L., Muxlow, M. R., and Neubig, R. R. (2010) Use of flow cytometric methods to quantify protein-protein interactions, *Curr Protoc Cytom Chapter 13*, Unit 13 11 11-15.
155. Zhang, J. H., Chung, T. D., and Oldenburg, K. R. (1999) A Simple Statistical Parameter for Use in Evaluation and Validation of High Throughput Screening Assays, *J Biomol Screen 4*, 67-73.
156. Bulut, V. N., Arslan, D., Ozdes, D., Soylak, M., and Tufekci, M. (2010) Preconcentration, separation and spectrophotometric determination of aluminium(III) in water samples and dialysis concentrates at trace levels with 8-hydroxyquinoline-cobalt(II) coprecipitation system, *J Hazard Mater 182*, 331-336.
157. Fazaeli, Y., Amini, M. M., Mohajerani, E., Sharbatdaran, M., and Torabi, N. (2010) Grafting aluminum(III) 8-hydroxyquinoline derivatives on MCM-41 mesoporous silica for tuning of the light emitting color, *J Colloid Interface Sci 346*, 384-390.
158. Kazi, T. G., Khan, S., Baig, J. A., Kolachi, N. F., Afridi, H. I., Kandhro, G. A., Kumar, S., and Shah, A. Q. (2009) Separation and preconcentration of aluminum in parenteral solutions and bottled mineral water using different analytical techniques, *J Hazard Mater 172*, 780-785.
159. Sullivan, D. M., Kehoe, D. F., and Smith, R. L. (1987) Measurement of trace levels of total aluminum in foods by atomic absorption spectrophotometry, *J Assoc Off Anal Chem 70*, 118-120.
160. Yokel, R. A. (2002) Aluminum chelation principles and recent advances, *Coordination Chemistry Reviews 228*, 97-113.
161. Arkin, M. R., and Whitty, A. (2009) The road less traveled: modulating signal transduction enzymes by inhibiting their protein-protein interactions, *Current Opinion in Chemical Biology 13*, 284-290.
162. Stebbins, J. L., De, S. K., Machleidt, T., Becattini, B., Vazquez, J., Kuntzen, C., Chen, L. H., Cellitti, J. F., Riel-Mehan, M., Emdadi, A., Solinas, G., Karin, M., and Pellecchia, M. (2008) Identification of a new

JNK inhibitor targeting the JNK-JIP interaction site, *Proc Natl Acad Sci U S A 105*, 16809-16813.
163. Reindl, W., Yuan, J., Kramer, A., Strebhardt, K., and Berg, T. (2008) Inhibition of polo-like kinase 1 by blocking polo-box domain-dependent protein-protein interactions, *Chem Biol 15*, 459-466.
164. Roehrl, M. H., Kang, S., Aramburu, J., Wagner, G., Rao, A., and Hogan, P. G. (2004) Selective inhibition of calcineurin-NFAT signaling by blocking protein-protein interaction with small organic molecules, *Proc Natl Acad Sci U S A 101*, 7554-7559.
165. Roehrl, M. H., Wang, J. Y., and Wagner, G. (2004) Discovery of small-molecule inhibitors of the NFAT--calcineurin interaction by competitive high-throughput fluorescence polarization screening, *Biochemistry 43*, 16067-16075.
166. Berg, T. (2008) Small-molecule inhibitors of protein-protein interactions, *Curr Opin Drug Discov Devel 11*, 666-674.
167. Yin, H., and Hamilton, A. D. (2005) Strategies for targeting protein-protein interactions with synthetic agents, *Angew Chem Int Ed Engl 44*, 4130-4163.
168. Breitenlechner, C. B., Bossemeyer, D., and Engh, R. A. (2005) Crystallography for protein kinase drug design: PKA and SRC case studies, *Biochim Biophys Acta 1754*, 38-49.
169. Morphy, R. (2010) Selectively nonselective kinase inhibition: striking the right balance, *J Med Chem 53*, 1413-1437.
170. Noble, M. E., Endicott, J. A., and Johnson, L. N. (2004) Protein kinase inhibitors: insights into drug design from structure, *Science 303*, 1800-1805.
171. Rabiller, M., Getlik, M., Kluter, S., Richters, A., Tuckmantel, S., Simard, J. R., and Rauh, D. (2010) Proteus in the world of proteins: conformational changes in protein kinases, *Arch Pharm (Weinheim) 343*, 193-206.
172. Zuccotto, F., Ardini, E., Casale, E., and Angiolini, M. (2010) Through the "gatekeeper door": exploiting the active kinase conformation, *J Med Chem 53*, 2681-2694.
173. Dorn, G. W., 2nd. (2009) GRK mythology: G-protein receptor kinases in cardiovascular disease, *J Mol Med 87*, 455-463.
174. Lodowski, D. T., Pitcher, J. A., Capel, W. D., Lefkowitz, R. J., and Tesmer, J. J. (2003) Keeping G proteins at bay: a complex between G protein-coupled receptor kinase 2 and Gbetagamma, *Science 300*, 1256-1262.
175. Tesmer, J. J., Tesmer, V. M., Lodowski, D. T., Steinhagen, H., and Huber, J. (2010) Structure of human G protein-coupled receptor kinase 2 in complex with the kinase inhibitor balanol, *J Med Chem 53*, 1867-1870.
176. Takeda. (2007) PCT/JP06318666.
177. Koide, K., Bunnage, M. E., Gomez Paloma, L., Kanter, J. R., Taylor, S. S., Brunton, L. L., and Nicolaou, K. C. (1995) Molecular design and biological activity of potent and selective protein kinase inhibitors related to balanol, *Chem Biol 2*, 601-608.

178. Huang, C. C., Yoshino-Koh, K., and Tesmer, J. J. (2009) A surface of the kinase domain critical for the allosteric activation of G protein-coupled receptor kinases, *J Biol Chem 284*, 17206-17215.
179. Lodowski, D. T., Barnhill, J. F., Pitcher, J. A., Capel, W. D., Lefkowitz, R. J., and Tesmer, J. J. (2003) Purification, crystallization and preliminary X-ray diffraction studies of a complex between G protein-coupled receptor kinase 2 and $G\beta_1\gamma_2$, *Acta Crystallogr D Biol Crystallogr 59*, 936-939.
180. Schuttelkopf, A. W., and van Aalten, D. M. (2004) PRODRG: a tool for high-throughput crystallography of protein-ligand complexes, *Acta Crystallogr D Biol Crystallogr 60*, 1355-1363.
181. Emsley, P., and Cowtan, K. (2004) Coot: model-building tools for molecular graphics, *Acta Crystallogr D Biol Crystallogr 60*, 2126-2132.
182. Murshudov, G. N., Vagin, A. A., and Dodson, E. J. (1997) Refinement of macromolecular structures by the maximum-likelihood method, *Acta Crystallogr D Biol Crystallogr 53*, 240-255.
183. Winn, M. D., Isupov, M. N., and Murshudov, G. N. (2001) Use of TLS parameters to model anisotropic displacements in macromolecular refinement, *Acta Crystallogr D Biol Crystallogr 57*, 122-133.
184. Chen, V. B., Arendall, W. B., 3rd, Headd, J. J., Keedy, D. A., Immormino, R. M., Kapral, G. J., Murray, L. W., Richardson, J. S., and Richardson, D. C. (2010) MolProbity: all-atom structure validation for macromolecular crystallography, *Acta Crystallogr D Biol Crystallogr 66*, 12-21.
185. Laskowski, R. A., MacArthur, M. W., Moss, D. S., and Thornton, J. M. (1993) PROCHECK: a program to check the stereochemical quality of protein structures, *J. Appl. Crystallogr. 26*, 283-291.
186. Singh, P., Wang, B., Maeda, T., Palczewski, K., and Tesmer, J. J. (2008) Structures of rhodopsin kinase in different ligand states reveal key elements involved in G protein-coupled receptor kinase activation, *J Biol Chem 283*, 14053-14062.
187. Papermaster, D. S. (1982) Preparation of antibodies to rhodopsin and the large protein of rod outer segments, *Methods Enzymol 81*, 240-246.
188. Mezzasalma, T. M., Kranz, J. K., Chan, W., Struble, G. T., Schalk-Hihi, C. l., Deckman, I. C., Springer, B. A., and Todd, M. J. (2007) Enhancing Recombinant Protein Quality and Yield by Protein Stability Profiling, *Journal of Biomolecular Screening 12*, 418-428.
189. Liu, Y., and Gray, N. S. (2006) Rational design of inhibitors that bind to inactive kinase conformations, *Nat Chem Biol 2*, 358-364.
190. Narayana, N., Diller, T. C., Koide, K., Bunnage, M. E., Nicolaou, K. C., Brunton, L. L., Xuong, N. H., Ten Eyck, L. F., and Taylor, S. S. (1999) Crystal structure of the potent natural product inhibitor balanol in complex with the catalytic subunit of cAMP-dependent protein kinase, *Biochemistry 38*, 2367-2376.
191. Breitenlechner, C. B., Friebe, W. G., Brunet, E., Werner, G., Graul, K., Thomas, U., Kunkele, K. P., Schafer, W., Gassel, M., Bossemeyer, D., Huber, R., Engh, R. A., and Masjost, B. (2005) Design and crystal

structures of protein kinase B-selective inhibitors in complex with protein kinase A and mutants, *J Med Chem 48*, 163-170.
192. Bonn, S., Herrero, S., Breitenlechner, C. B., Erlbruch, A., Lehmann, W., Engh, R. A., Gassel, M., and Bossemeyer, D. (2006) Structural analysis of protein kinase A mutants with Rho-kinase inhibitor specificity, *J Biol Chem 281*, 24818-24830.
193. Holdgate, G. A., and Ward, W. H. (2005) Measurements of binding thermodynamics in drug discovery, *Drug Discov Today 10*, 1543-1550.
194. Boguth, C. A., Singh, P., Huang, C. C., and Tesmer, J. J. (2010) Molecular basis for activation of G protein-coupled receptor kinases, *EMBO J*.
195. Pitcher, J. A., Hall, R. A., Daaka, Y., Zhang, J., Ferguson, S. S., Hester, S., Miller, S., Caron, M. G., Lefkowitz, R. J., and Barak, L. S. (1998) The G protein-coupled receptor kinase 2 is a microtubule-associated protein kinase that phosphorylates tubulin, *J Biol Chem 273*, 12316-12324.
196. Luttrell, L. M., and Lefkowitz, R. J. (2002) The role of β-arrestins in the termination and transduction of G-protein-coupled receptor signals, *J Cell Sci 115*, 455-465.
197. Lohse, M. J., Benovic, J. L., Codina, J., Caron, M. G., and Lefkowitz, R. J. (1990) β-Arrestin: a protein that regulates β-adrenergic receptor function, *Science 248*, 1547-1550.
198. Attramadal, H., Arriza, J. L., Aoki, C., Dawson, T. M., Codina, J., Kwatra, M. M., Snyder, S. H., Caron, M. G., and Lefkowitz, R. J. (1992) β-arrestin2, a novel member of the arrestin/β-arrestin gene family, *J Biol Chem 267*, 17882-17890.
199. Sterne-Marr, R., and Benovic, J. L. (1995) Regulation of G protein-coupled receptors by receptor kinases and arrestins, *Vitam Horm 51*, 193-234.
200. Goodman, O. B., Jr., Krupnick, J. G., Santini, F., Gurevich, V. V., Penn, R. B., Gagnon, A. W., Keen, J. H., and Benovic, J. L. (1996) β-arrestin acts as a clathrin adaptor in endocytosis of the β2-adrenergic receptor, *Nature 383*, 447-450.
201. Daaka, Y., Luttrell, L. M., Ahn, S., Della Rocca, G. J., Ferguson, S. S., Caron, M. G., and Lefkowitz, R. J. (1998) Essential role for G protein-coupled receptor endocytosis in the activation of mitogen-activated protein kinase, *J Biol Chem 273*, 685-688.
202. Perry, S. J., and Lefkowitz, R. J. (2002) Arresting developments in heptahelical receptor signaling and regulation, *Trends Cell Biol 12*, 130-138.
203. Krispel, C. M., Chen, D., Melling, N., Chen, Y. J., Martemyanov, K. A., Quillinan, N., Arshavsky, V. Y., Wensel, T. G., Chen, C. K., and Burns, M. E. (2006) RGS expression rate-limits recovery of rod photoresponses, *Neuron 51*, 409-416.
204. Hanks, S. K., and Hunter, T. (1995) Protein kinases 6. The eukaryotic protein kinase superfamily: kinase (catalytic) domain structure and classification, *FASEB J 9*, 576-596.

205. Kostich, M., English, J., Madison, V., Gheyas, F., Wang, L., Qiu, P., Greene, J., and Laz, T. M. (2002) Human members of the eukaryotic protein kinase family, *Genome Biol 3*, RESEARCH0043.
206. Bouvier, M., Hausdorff, W. P., De Blasi, A., O'Dowd, B. F., Kobilka, B. K., Caron, M. G., and Lefkowitz, R. J. (1988) Removal of phosphorylation sites from the beta 2-adrenergic receptor delays onset of agonist-promoted desensitization, *Nature 333*, 370-373.
207. Pippig, S., Andexinger, S., Daniel, K., Puzicha, M., Caron, M. G., Lefkowitz, R. J., and Lohse, M. J. (1993) Overexpression of beta-arrestin and beta-adrenergic receptor kinase augment desensitization of beta 2-adrenergic receptors, *J Biol Chem 268*, 3201-3208.
208. Kong, G., Penn, R., and Benovic, J. L. (1994) A beta-adrenergic receptor kinase dominant negative mutant attenuates desensitization of the beta 2-adrenergic receptor, *J Biol Chem 269*, 13084-13087.
209. Kiuchi, K., Shannon, R. P., Komamura, K., Cohen, D. J., Bianchi, C., Homcy, C. J., Vatner, S. F., and Vatner, D. E. (1993) Myocardial beta-adrenergic receptor function during the development of pacing-induced heart failure, *J Clin Invest 91*, 907-914.
210. Vatner, D. E., Sato, N., Ishikawa, Y., Kiuchi, K., Shannon, R. P., and Vatner, S. F. (1996) Beta-adrenoceptor desensitization during the development of canine pacing-induced heart failure, *Clin Exp Pharmacol Physiol 23*, 688-692.
211. Ping, P., Anzai, T., Gao, M., and Hammond, H. K. (1997) Adenylyl cyclase and G protein receptor kinase expression during development of heart failure, *Am J Physiol 273*, H707-717.
212. Bristow, M. R., Ginsburg, R., Umans, V., Fowler, M., Minobe, W., Rasmussen, R., Zera, P., Menlove, R., Shah, P., Jamieson, S., and et al. (1986) Beta 1- and beta 2-adrenergic-receptor subpopulations in nonfailing and failing human ventricular myocardium: coupling of both receptor subtypes to muscle contraction and selective beta 1-receptor down- regulation in heart failure, *Circ Res 59*, 297-309.
213. Ungerer, M., Parruti, G., Bohm, M., Puzicha, M., DeBlasi, A., Erdmann, E., and Lohse, M. J. (1994) Expression of beta-arrestins and beta-adrenergic receptor kinases in the failing human heart, *Circ Res 74*, 206-213.
214. Rockman, H. A., Chien, K. R., Choi, D. J., Iaccarino, G., Hunter, J. J., Ross, J., Jr., Lefkowitz, R. J., and Koch, W. J. (1998) Expression of a beta-adrenergic receptor kinase 1 inhibitor prevents the development of myocardial failure in gene-targeted mice, *Proc Natl Acad Sci U S A 95*, 7000-7005.
215. Harding, V. B., Jones, L. R., Lefkowitz, R. J., Koch, W. J., and Rockman, H. A. (2001) Cardiac beta ARK1 inhibition prolongs survival and augments beta blocker therapy in a mouse model of severe heart failure, *Proc Natl Acad Sci U S A 98*, 5809-5814.
216. Rockman, H. A., Koch, W. J., and Lefkowitz, R. J. (2002) Seven-transmembrane-spanning receptors and heart function, *Nature 415*, 206-212.

217. Lymperopoulos, A., Rengo, G., Funakoshi, H., Eckhart, A. D., and Koch, W. J. (2007) Adrenal GRK2 upregulation mediates sympathetic overdrive in heart failure, *Nat Med 13*, 315-323.
218. Lymperopoulos, A., Rengo, G., Gao, E., Ebert, S. N., Dorn, G. W., 2nd, and Koch, W. J. (2010) Reduction of sympathetic activity via adrenal-targeted GRK2 gene deletion attenuates heart failure progression and improves cardiac function after myocardial infarction, *J Biol Chem 285*, 16378-16386.
219. Benovic, J. L., Stone, W. C., Caron, M. G., and Lefkowitz, R. J. (1989) Inhibition of the beta-adrenergic receptor kinase by polyanions, *J Biol Chem 264*, 6707-6710.
220. Benovic, J. L. (1991) Purification and characterization of beta-adrenergic receptor kinase, *Methods Enzymol 200*, 351-362.
221. Kassack, M. U. (2000) G-protein coupled receptor kinases and their inhibitors, *Expert Opinion on Therapeutic Patents 10*, 917-928.
222. Benovic, J. L., Onorato, J., Lohse, M. J., Dohlman, H. G., Staniszewski, C., Caron, M. G., and Lefkowitz, R. J. (1990) Synthetic peptides of the hamster β_2-adrenoceptor as substrates and inhibitors of the β-adrenoceptor kinase, *Br J Clin Pharmacol 30 Suppl 1*, 3S-12S.
223. Winstel, R., Ihlenfeldt, H. G., Jung, G., Krasel, C., and Lohse, M. J. (2005) Peptide inhibitors of G protein-coupled receptor kinases, *Biochem Pharmacol 70*, 1001-1008.
224. Kulanthaivel, P., Hallock, Y. F., Boros, C., Hamilton, S. M., Janzen, W. P., Ballas, L. M., Loomis, C. R., and Jiang, J. B. (1993) Balanol: a novel and potent inhibitor of protein kinase C from the fungus *Verticillium balanoides*, *J. Am. Chem. Soc. 115*, 6452-6453.
225. Akamine, P., Madhusudan, Brunton, L. L., Ou, H. D., Canaves, J. M., Xuong, N. H., and Taylor, S. S. (2004) Balanol analogues probe specificity determinants and the conformational malleability of the cyclic 3',5'-adenosine monophosphate-dependent protein kinase catalytic subunit, *Biochemistry 43*, 85-96.
226. Pande, V., Ramos, M. J., and Gago, F. (2008) The Protein kinase inhibitor balanol: structure-activity relationships and structure-based computational studies, *Anticancer Agents Med Chem 8*, 638-645.
227. Lee, J. F., Stovall, G. M., and Ellington, A. D. (2006) Aptamer therapeutics advance, *Curr Opin Chem Biol 10*, 282-289.
228. Mayer, G., Wulffen, B., Huber, C., Brockmann, J., Flicke, B., Neumann, L., Hafenbradl, D., Klebl, B. M., Lohse, M. J., Krasel, C., and Blind, M. (2008) An RNA molecule that specifically inhibits G-protein-coupled receptor kinase 2 in vitro, *Rna 14*, 524-534.
229. Johnson, L. N. (2009) Protein kinase inhibitors: contributions from structure to clinical compounds, *Q Rev Biophys 42*, 1-40.
230. Kluter, S., Grutter, C., Naqvi, T., Rabiller, M., Simard, J. R., Pawar, V., Getlik, M., and Rauh, D. (2010) Displacement assay for the detection of stabilizers of inactive kinase conformations, *J Med Chem 53*, 357-367.

231. Nagar, B., Bornmann, W. G., Pellicena, P., Schindler, T., Veach, D. R., Miller, W. T., Clarkson, B., and Kuriyan, J. (2002) Crystal structures of the kinase domain of c-Abl in complex with the small molecule inhibitors PD173955 and imatinib (STI-571), *Cancer Res 62*, 4236-4243.
232. Hafner, M., Schmitz, A., Grune, I., Srivatsan, S. G., Paul, B., Kolanus, W., Quast, T., Kremmer, E., Bauer, I., and Famulok, M. (2006) Inhibition of cytohesins by SecinH3 leads to hepatic insulin resistance, *Nature 444*, 941-944.
233. McGovern, S. L., Caselli, E., Grigorieff, N., and Shoichet, B. K. (2002) A common mechanism underlying promiscuous inhibitors from virtual and high-throughput screening, *J Med Chem 45*, 1712-1722.
234. Cohen, P. (2002) Protein kinases--the major drug targets of the twenty-first century?, *Nat Rev Drug Discov 1*, 309-315.
235. Smyth, L. A., and Collins, I. (2009) Measuring and interpreting the selectivity of protein kinase inhibitors, *J Chem Biol 2*, 131-151.
236. Kenski, D. M., Zhang, C., von Zastrow, M., and Shokat, K. M. (2005) Chemical genetic engineering of G protein-coupled receptor kinase 2, *J Biol Chem 280*, 35051-35061.